

Comprehensive Imaging of Ischemic Stroke with Multisection CT¹

Bernd F. Tomandl, MD • Ernst Klotz, Dipl Phys • Rene Handschu, MD
Brigitte Stemper, MD • Frank Reinhardt, MD • Walter J. Huk, MD
K.E. Eberhardt, MD • Suzanne Fateh-Moghadam, MD

Computed tomography (CT) is an established tool for the diagnosis of ischemic or hemorrhagic stroke. Nonenhanced CT can help exclude hemorrhage and detect “early signs” of infarction but cannot reliably demonstrate irreversibly damaged brain tissue in the hyperacute stage of ischemic stroke. Further evaluation of patients with ischemic stroke should include differentiation between reversible and irreversible brain damage, which is essential for choosing an appropriate therapy. Perfusion CT provides information about brain perfusion, which permits differentiation of irreversibly damaged brain tissue from reversibly impaired “tissue at risk.” CT angiography can help detect stenosis or occlusion of extra- and intracranial arteries. Multisection CT allows the combined use of all three imaging modalities—nonenhanced CT, perfusion CT, and CT angiography—to rapidly obtain comprehensive information regarding the extent of ischemic damage in acute stroke patients. Specific patterns of findings are typically seen in ischemic stroke and can be analyzed more accurately with the combined use of multisection CT and MR imaging. Nevertheless, prospective studies involving a large number of patients will be needed to ascertain the treatment of choice for patients with each of these patterns of findings.

©RSNA, 2003

Abbreviations: CBF = cerebral blood flow, CBV = cerebral blood volume, ICA = internal carotid artery, MCA = middle cerebral artery, MIP = maximum intensity projection, MTT = mean transit time, ROI = region of interest, SSD = shaded surface display, TAC = time-attenuation curve, TTP = time to peak, VR = volume rendering, 3D = three-dimensional

Index terms: Brain, CT, 10.1211 • Brain, infarction, 10.781 • Brain, ischemia, 10.781

RadioGraphics 2003; 23:565–592 • **Published online** 10.1148/rg.233025036

¹From the Division of Neuroradiology, Department of Neurosurgery (B.F.T., W.J.H., K.E.E.) and the Departments of Neurology (R.H., B.S., F.R.) and Internal Medicine II (S.F.M.), University of Erlangen-Nuremberg, Schwabachanlage 6, D-91054 Erlangen, Germany; and Siemens Medical Solutions, Forchheim, Germany (E.K.). Recipient of a Magna Cum Laude award for an education exhibit at the 2001 RSNA scientific assembly. Received February 26, 2002; revision requested April 24; final revision received November 14; accepted November 15. **Address correspondence to** B.F.T. (e-mail: tomandl@neuroradiologie-erlangen.de).

©RSNA, 2003

Introduction

Nonenhanced computed tomography (CT) was used until the late 1980s primarily to exclude hemorrhage in patients with acute stroke. Requirements for diagnostic imaging in patients with ischemic stroke changed as a result of the 1995 study by the National Institute of Neurological Disorders and Stroke (NINDS) (1,2). Thrombolysis was introduced for the treatment of ischemic lesions of the middle cerebral artery (MCA) territory. A recently published meta-analysis by Wardlaw (3) summarizes the results of all studies in which thrombolytic agents were used to treat acute ischemia within 3–6 hours after the acute event. This meta-analysis showed a significant reduction in the number of patients with poor functional outcome at the end of follow-up. However, there was also a higher risk of hemorrhage and death within the 1st 10 days after treatment (3). This risk increased as the time interval between the onset of symptoms and thrombolytic therapy increased. Thus, patients are more likely to have a good outcome when treated within 3 hours than between 3 and 6 hours after the acute event (3-6). Therefore, the primary purpose of diagnostic imaging is to ensure selection of the appropriate patients for thrombolytic therapy to reduce severe complications.

For this purpose, diagnostic imaging of acute stroke should reliably help (*a*) exclude intracranial hemorrhage, (*b*) differentiate between irreversibly affected brain tissue (“dead brain”) and reversibly impaired tissue (“tissue at risk”), which might benefit from early treatment, and (*c*) identify stenosis or occlusion of major extra- and intracranial arteries. Tissue at risk, or “penumbra,” is defined as an area of markedly reduced perfusion with loss of function of still viable neurons (7,8). Timely reperfusion of this tissue may prevent cell death and help reestablish normal function.

Because thrombolysis of large areas of irreversibly affected brain tissue carries a high risk of hemorrhage, patients with infarction that affects more than one-third of the MCA territory should not undergo thrombolysis (9).

At nonenhanced CT, “early signs” (discussed later) can include cerebral infarction but usually not before 2–3 hours after the onset of symptoms. However, more reliable imaging techniques are required to facilitate the decision to perform thrombolysis in selected patients (10). Now, after the introduction of spiral CT in the early 1990s, these techniques include perfusion CT, in which dynamic CT is used to track a bolus of contrast material as it travels through the brain, and CT angiography for the visualization of intracranial arteries. Multisection CT is superior to single-section spiral CT in combining all these techniques in a time-optimized protocol for comprehensive imaging of stroke patients in emergency situations.

In this article, we introduce a stroke protocol that combines nonenhanced CT, perfusion CT, and CT angiography performed with a four-detector row multisection CT scanner. This protocol has been used in our department since spring 2000 as a routine method for evaluating patients with symptoms of ischemic stroke ($n = 85$). We describe each of the three imaging components of the protocol and discuss the implications of the combined application of all three components for diagnosis as well as typical patterns of findings in affected patients. We also discuss some possible shortcomings of multisection CT and briefly compare the use of CT and MR imaging in ischemic stroke.

Multisection CT Techniques

General Considerations

Four-detector row multisection helical CT was introduced in 1998 and improved temporal and spatial resolution significantly by allowing four sections to be obtained simultaneously during each gantry rotation. This advance, together with a short rotation time of 0.5 seconds, meant that a routine examination could be performed up to eight times faster than with single-section spiral CT (11,12). Equipped with up to 16 detector rows, most modern scanners acquire data even more quickly, allowing not only isotropic examination of large volumes such as the entire vascular tree from the aortic arch to the intracranial vessels, but also the creation of multiplanar refor-

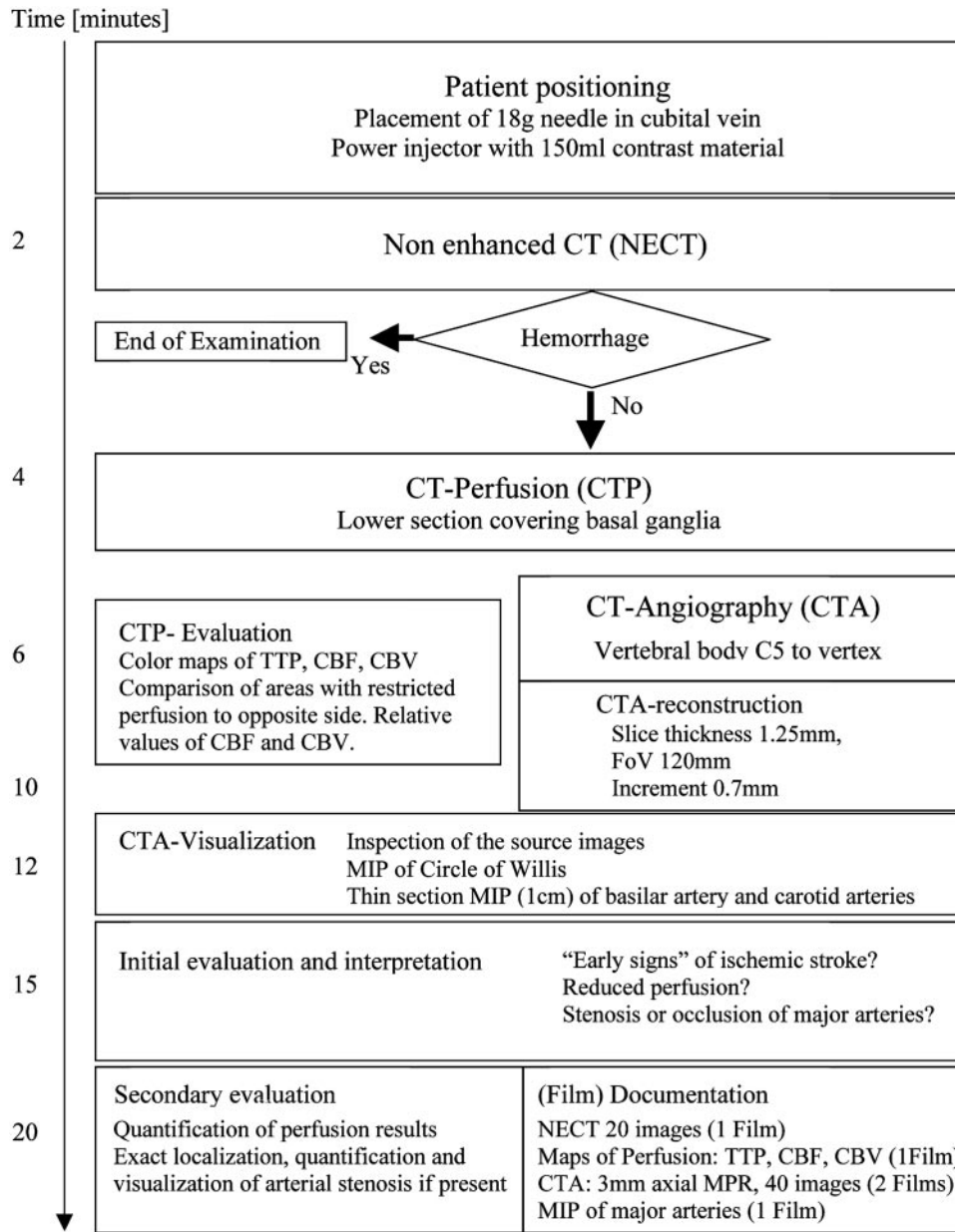


Figure 1. Chart illustrates a protocol for evaluating stroke patients with multi-section CT and the average time needed to complete each step. Note that perfusion CT data are being evaluated while CT angiograms are being acquired and reformatted. *CBF* = cerebral blood flow, *CBV* = cerebral blood volume, *MIP* = maximum intensity projection, *MPR* = multiplanar reformatting, *TTP* = time to peak.

matted images with identical spatial resolution (4,13). The advantages of multisection CT for vascular imaging of stroke patients are obvious. For example, the investigation of a region including the carotid bifurcation and intracranial vessels can be performed in less than 20 seconds. For perfusion CT, serial CT is performed after bolus administration of contrast material. The maximum thickness of the section depends on the number of detector rows available. Typically, a 2-cm-thick

section can be acquired with a four-row multisection CT scanner. With 16-row scanners, sections about 3 cm in thickness can be obtained with perfusion CT. Whole brain perfusion studies are not yet possible.

Figure 1 illustrates the workflow of a standardized stroke protocol that combines nonenhanced CT, perfusion CT, and CT angiography. The

studies and postprocessing procedures were performed with a four-row multisection CT scanner (Volume Zoom; Siemens Medical Solutions, Forchheim, Germany) equipped with a workstation for three-dimensional (3D) postprocessing (Wizard workstation, Syngo user interface, Version VA40a, Siemens Medical Solutions) and an integrated software package for the evaluation of perfusion CT data. The protocol is optimized for this particular scanner and can easily be adapted to any multisection CT equipment.

The main goal of using this protocol was to complete data acquisition and postprocessing in a minimal amount of time.

After intracranial hemorrhage is excluded with nonenhanced CT, perfusion CT is immediately started, followed by CT angiography. The evaluation of the perfusion CT data occurs simultaneously with the acquisition and reformatting of the CT angiography source images. Data acquisition with the three studies is generally completed within 7–8 minutes. Multiplanar reformatting and postprocessing of the CT angiograms with maximum intensity projection (MIP) requires another 4–6 minutes. With a mean time of 12.6 minutes (range, 11–14 minutes) required for the evaluation of all data, therapeutic decisions concerning thrombolysis can be made in less than 15 minutes. At least 10 more minutes are needed to produce film images and perform detailed evaluation of arterial stenosis with 3D images.

Nonenhanced CT

Data Acquisition.—Nonenhanced CT was performed with the following parameters: 120 kVp, 300 mAs, and a section thickness of 4 mm for the posterior fossa and 8 mm for the supratentorial region. This examination usually took less than 1 minute.

Image Interpretation.—When intracerebral hemorrhage or other lesions (eg, tumor, infection) that cause acute neurologic deficits are excluded at initial nonenhanced CT, an ischemic lesion must be assumed. Ischemia of the MCA

territory can be assumed if early signs of infarction are identified on nonenhanced CT scans. These early signs include:

1. Obscuration of the lentiform nucleus. Increasing hypoattenuation due to cytotoxic edema can be observed within 2 hours after onset (14). Because the lenticulostriate branches of the MCA are end-vessels, the lentiform nucleus is prone to early irreversible damage after proximal MCA occlusion.

2. Insular ribbon sign. Hypoattenuation of the insular cortex in the early stage of MCA occlusion can be explained by its watershed position far from the collateral supply of both the anterior and posterior cerebral arteries, which leads to early irreversible damage (15).

3. Hyperattenuating (“hyperdense”) media sign. If the MCA is occluded by a fresh thrombus, it appears hyperattenuating relative to the normal contralateral MCA at nonenhanced CT (16,17). Unlike the other early signs, the hyperattenuating media sign indicates occlusion of the MCA, not infarction within the MCA territory. This sign can be seen within 90 minutes after the acute event (18). According to Leys et al (19), its specificity is nearly 100%, but its sensitivity is only about 30%. Thrombosis of more peripheral branches of the MCA may also be suspected on the basis of hyperattenuating “dots” (20).

4. Normal findings in the affected brain tissue within the 1st 2-3 hours after the onset of symptoms in most cases. Over time, irreversibly damaged brain tissue can be recognized as areas of hypoattenuation with effacement of adjacent sulci (21).

These early signs indicate occlusion of the MCA; however, within the 1st 3 hours after onset of stroke they do not provide sufficient information about the extent of irreversibly damaged brain tissue, which is essential to avoid hemorrhage during thrombolysis of ischemic lesions (22). In the second part of the European Cooperative Acute Stroke Study (ECASS II), specially trained neuroradiologic experts evaluated the extent of early signs within the 1st 6 hours after the onset of ischemic symptoms. The accuracy of predicting the exact volume of affected brain tissue was only 76% (9). This outcome emphasizes

the need for more reliable imaging techniques that can help determine the extent of both irreversibly damaged brain tissue and tissue at risk to avoid unnecessary thrombolytic therapy.

Perfusion CT

Brain Perfusion.—Perfusion of normal brain tissue is maintained within a narrow range by autoregulation of the cerebral vasculature. Normal blood flow in human gray matter is about 50–60 mL/100 g/min (23). In cases of occlusion of a major artery like the MCA, the survival of brain tissue depends on the minimum necessary collateral supply from leptomeningeal anastomoses. On the basis of animal studies, a three-compartment model with respect to thresholds for the function and survival of ischemic tissue was suggested (24,25).

1. At a cerebral blood flow (CBF) of 35 mL/100 g/min or less (ie, approximately 50%–60% of normal values), protein synthesis within neurons ceases completely (26). In this oligemic stage, tissue can survive as long as CBF is not further reduced.

2. At a CBF of 20 mL/100 g/min or less (ie, approximately 30%–40% of normal values), synaptic transmission between neurons is disturbed, leading to loss of function of still viable neurons (24). Ischemic brain tissue that is “living” under these conditions adjacent to already irreversibly damaged tissue is defined as tissue at risk.

3. At a CBF of 10 mL/100 g/min or less (ie, <20% of normal values), irreversible cell death occurs (7).

Reperfusion of tissue at risk within a therapeutic window of 3 hours or even more can lead to complete regeneration of neuronal function. The phrase *time is brain* refers to the fact that the extent of irreversibly damaged brain tissue increases with the duration of ischemia (27,28).

Typical parameters used to describe cerebral perfusion include:

1. Mean transit time (MTT), that is, the time between arterial inflow and venous outflow.
2. Time to peak (TTP), which is often calculated in perfusion CT studies and represents the

time from the beginning of contrast material injection to maximum (peak) enhancement within an intracerebral region of interest (ROI).

3. Cerebral blood volume (CBV), that is, the volume of blood per unit of brain mass. Normal CBV is about 4–5 mL/100 g (29). Under normal conditions, the relationship between CBF and CBV is expressed by the equation $CBF \times MTT = CBV$.

When the capillary bed dilates in the early stage of ischemia, CBV will remain unchanged or even increase despite a decrease in CBF. When the mechanisms of autoregulation can no longer compensate for a further reduction in CBF, CBV will also decrease. Therefore, simultaneous analysis of CBF and CBV as calculated from perfusion CT data is necessary to predict the volume of irreversibly damaged brain tissue and thus develop a prognosis for ischemic stroke (30,31).

Data Acquisition.—With single-section CT scanners, examination is limited to a 1-cm-thick section. With multisection CT scanners, a 2–3-cm-thick section can be examined. Depending on detector configuration, 2–4 sections with a thickness of 5,6,8,10, or 12 mm can be obtained. In our protocol, two adjacent 10-mm-thick sections (80 kVp, 180 mAs) were obtained per second for 37 seconds. A better spatial resolution can be obtained with four 5-mm-thick sections, but at the cost of twice the radiation dose for the same signal-to-noise ratio.

Because whole brain perfusion CT is not yet possible, the anatomic region that clinical symptoms indicate is most likely affected by ischemia must be selected for the examination. When MCA occlusion is suspected, the level of the basal ganglia is adjusted. Then the bolus of contrast material is injected, and subsequent changes in brain tissue attenuation are monitored during the transit time of approximately 5 seconds with high-temporal-resolution dynamic CT, obtaining one

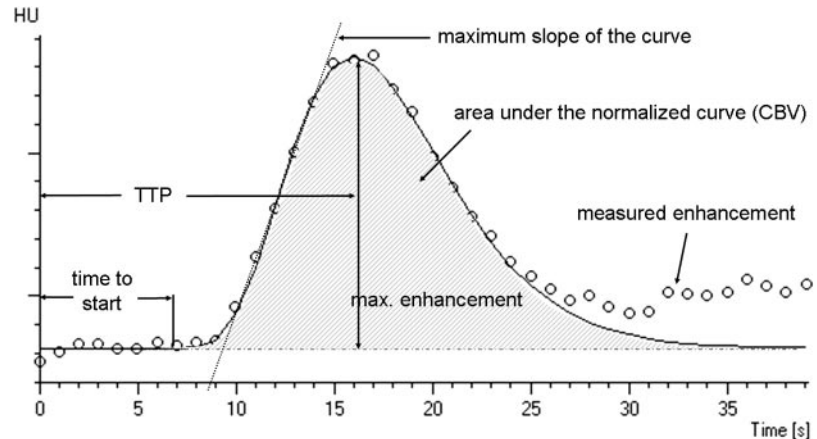


Figure 2. Graph illustrates a TAC plotted from perfusion CT data obtained in normal brain tissue. From this curve, per-voxel hemodynamic variables are calculated for TTP, CBF, and CBV. TTP is the time from the start of injection until maximum contrast enhancement is reached. However, some authors prefer to measure TTP from the beginning of enhancement by subtracting “time to start” (ie, the time between the start of injection and the start of enhancement). CBF can be estimated from the “maximum slope” of the curve. CBV is calculated from the area under the normalized curve and can also be estimated from the maximum enhancement compared with that of a reference vessel (eg, intracranial artery, superior sagittal sinus).

image per second. We injected 40 mL of contrast material (Ultravist 300; Schering, Berlin, Germany) at a flow rate of 8 mL/sec with a power injector (EnVision CT injector; Medrad, Indianapolis, Pa).

The semiautomatic postprocessing method used in our protocol delivers color maps of TTP, CBF, and CBV in less than 1 minute (Syngo Perfusion CT, Version VA40c, Siemens Medical Solutions) (32). User interaction is restricted to accepting certain parameters that are automatically proposed by the software. With use of this fast evaluation algorithm, postprocessing of perfusion CT scans can be performed during the data acquisition and image reformatting stages of the CT angiographic examination that follows.

Basic Principles of Perfusion CT and Postprocessing.—The rapid bolus injection of contrast material causes transient changes in enhancement as it travels through the cerebral vas-

culature. These changes are linearly proportional to the concentration of the contrast agent. With dynamic CT techniques, these changes can be graphed as regional time-attenuation curves (TACs) for every voxel. From these TACs, TTP or MTT, CBF, and CBV can be calculated (Fig 2).

TTP and MTT are both very sensitive to any kind of vascular disease, such as high-grade stenosis of the carotid artery. However, neither parameter is sufficient for the assessment of the severity of an ischemic process in its early stage because intact cerebrovascular autoregulation will maintain CBF by means of dilatation of the capillary bed even with reduced systemic blood pressure. Therefore, it is not possible to give a precise threshold of TTP or MTT that defines the volume of irreversibly damaged brain tissue (30,33).

Different mathematical approaches for the calculation of perfusion parameters can be used to evaluate perfusion CT data. These techniques are based on the indicator dilution principle, whereby a known amount of an indicator (contrast material) is injected into a cubital vein and its concen-

tration in an intracranial vessel is measured against time. Values for CBF and CBV can be derived from the resulting TAC with use of mathematical modeling. The postprocessing software we used is based on the maximum slope model of perfusion, in which the maximum slope of the TAC is used to calculate CBF (32,34,35). CBV values are calculated from the maximum enhancement ratio (ie, the maximum enhancement of the TAC in a given region compared with that of the superior sagittal sinus) (32,36,37). This approach has proved to be very robust, insensitive to motion, and clinically practical and requires no recirculation correction or operator decisions, which might bias reproducibility (35,38,39). The evaluation procedure that has been described in detail by Klotz and Konig (32) can be completed in less than 1 minute.

The maximum slope model requires a very rapid bolus injection of contrast material. A delayed appearance of the contrast material leads to a decrease in the maximum slope of the TAC, and absolute values for CBF will be underestimated. In addition, due to partial volume effects inherent in 5–10-mm-thick sections, the selective calculation of absolute perfusion parameters for gray and white matter will be nearly impossible. Therefore, comparing the values for CBF and CBV in the normal and affected hemispheres is a safer approach than relying on absolute values for CBF, which are prone to artifacts, and still allows quantitative data interpretation.

In our protocol, the contrast material was injected at a flow rate of 8 mL/sec through an 18-gauge intravenous needle to achieve rapid bolus injection. None of the 85 patients included in our study experienced any side effects or discomfort during this procedure. However, the creation of satisfactory color maps and the calculation of relative values for CBF and CBV are also possible with a 20-gauge needle at a flow rate of 5 mL/sec, despite an increase in image “noise” compared with higher flow rates. This lower flow rate (5 mL/sec) is independent of the type of algorithm (maximum slope versus deconvolution model) used for postprocessing (40). If a dual-piston power injector is available, the injection of 36 mL

of contrast material at a flow rate of 6 mL/sec followed by the injection of 40 mL of saline flush at the same flow rate makes it possible to obtain a bolus that is sufficiently short to meet the criteria of our protocol (Konig M, personal communication).

Deconvolution analysis is an alternative approach proposed by Axel (41), who developed the idea of perfusion CT as early as 1980. This approach is based on the regional MTT, which is calculated by deconvolving the TAC with respect to an arterial input function, and was recently introduced into a variety of implementations (42,43). According to the central volume principle, CBF is simply calculated from CBV or MTT. Initial reports showed the feasibility of this technique (44) and its usefulness in imaging patients with ischemic stroke (31). With flow rates of 4–5 mL/sec, the technique should theoretically provide absolute values for CBF and CBV (43). In practice, however, it is not completely free from a number of variables, such as the choice of the input artery and the recirculation correction, which are prone to artificial changes.

A detailed description of the different methods for calculating perfusion parameters is beyond the scope of this article. However, it should be kept in mind that all approaches are subject to inherent limitations and systematic errors, particularly in cases of acute stroke in which the vascular network has gone through complex adaptations and changes before the acute event. Therefore, an assessment of cerebral perfusion based on absolute values for CBF and CBV derived from perfusion CT studies should be made only with caution (45). Because of these methodologic problems, the definition of the tissue at risk in recent perfusion CT studies has generally been based on relative values for CBF and CBV independent of the model used for analysis (30,31).

Image Interpretation and Analysis.—For the evaluation of perfusion CT data, values are calculated for TTP or MTT, CBF, and CBV (Fig 3).

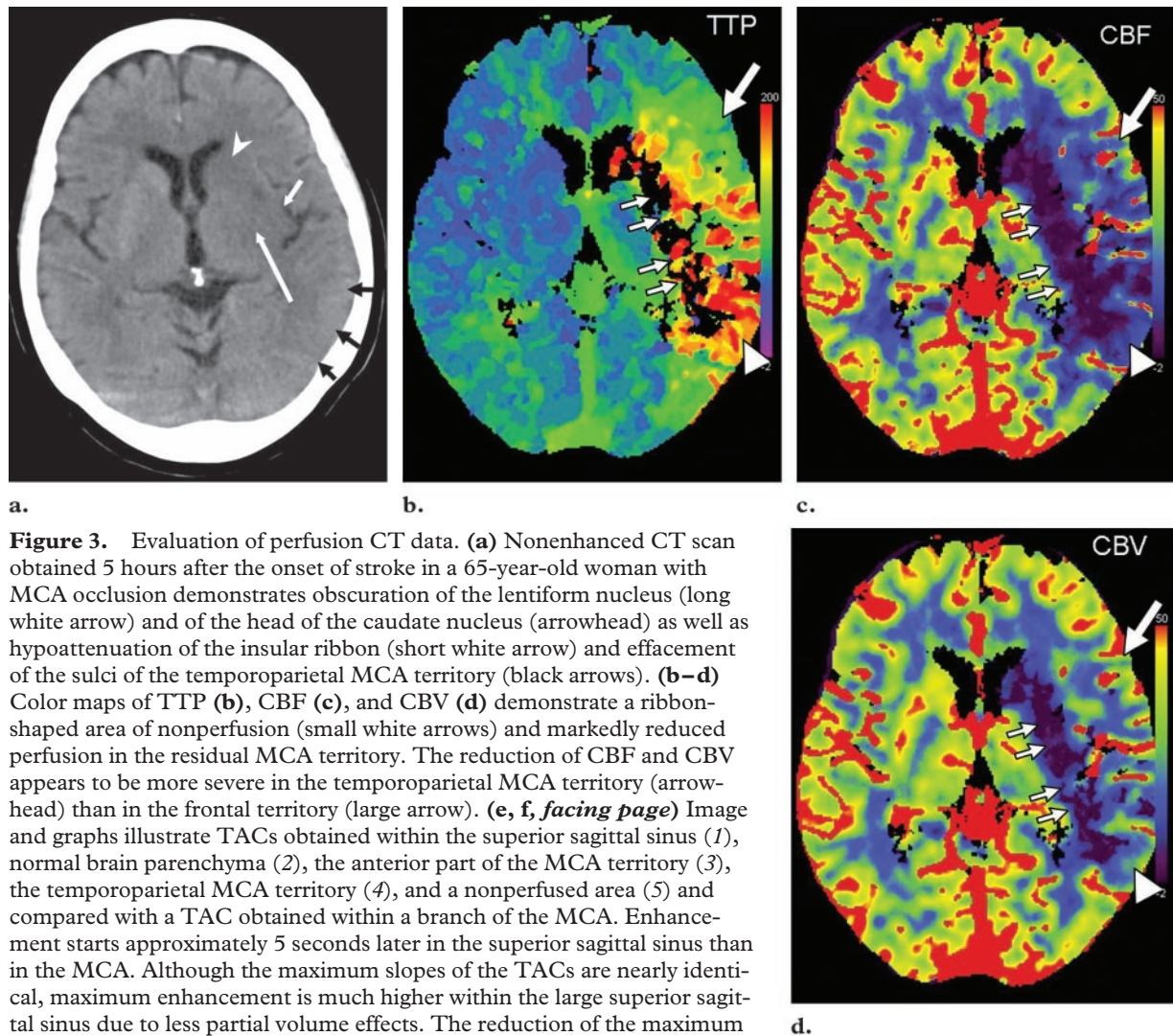
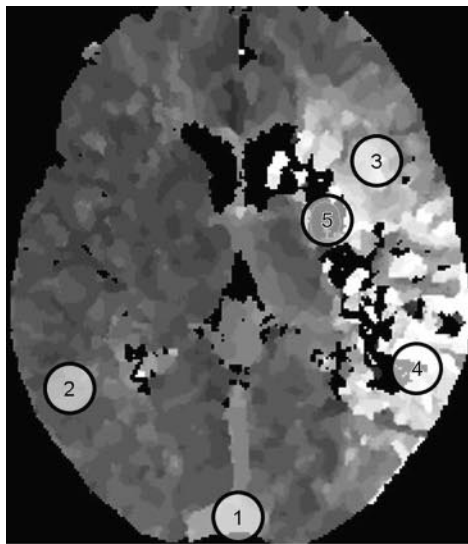
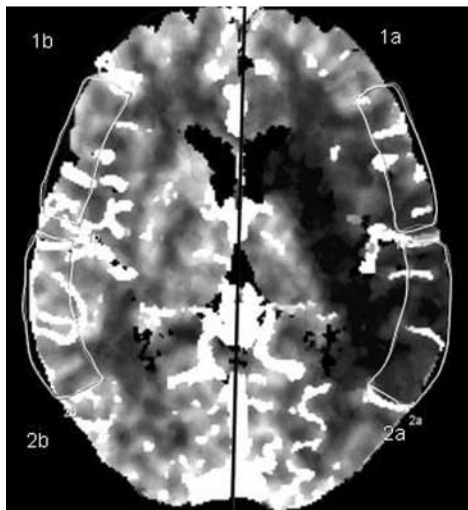
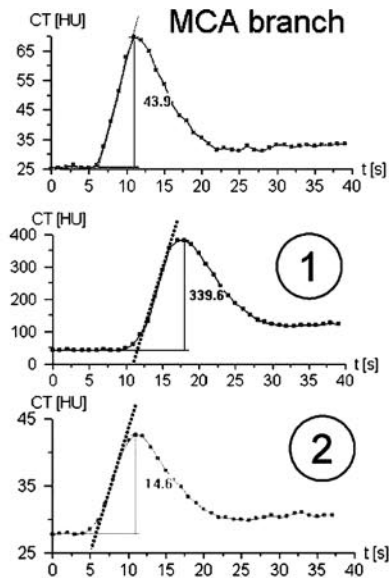


Figure 3. Evaluation of perfusion CT data. **(a)** Nonenhanced CT scan obtained 5 hours after the onset of stroke in a 65-year-old woman with MCA occlusion demonstrates obscuration of the lentiform nucleus (long white arrow) and of the head of the caudate nucleus (arrowhead) as well as hypoattenuation of the insular ribbon (short white arrow) and effacement of the sulci of the temporoparietal MCA territory (black arrows). **(b–d)** Color maps of TTP **(b)**, CBF **(c)**, and CBV **(d)** demonstrate a ribbon-shaped area of nonperfusion (small white arrows) and markedly reduced perfusion in the residual MCA territory. The reduction of CBF and CBV appears to be more severe in the temporoparietal MCA territory (arrowhead) than in the frontal territory (large arrow). **(e, f, facing page)** Image and graphs illustrate TACs obtained within the superior sagittal sinus (1), normal brain parenchyma (2), the anterior part of the MCA territory (3), the temporoparietal MCA territory (4), and a nonperfused area (5) and compared with a TAC obtained within a branch of the MCA. Enhancement starts approximately 5 seconds later in the superior sagittal sinus than in the MCA. Although the maximum slopes of the TACs are nearly identical, maximum enhancement is much higher within the large superior sagittal sinus due to less partial volume effects. The reduction of the maximum slope in the anterior part of the MCA territory compared with the superior sagittal sinus and the normal brain parenchyma is compatible with moderately reduced blood flow. There is further reduction of the maximum slope and decreased maximum enhancement in the temporoparietal MCA territory compared with the normal brain parenchyma. At follow-up, this area was infarcted. The TAC for the nonperfused area shows no enhancement, a finding that indicates irreversible infarction. **(g, facing page)** Image shows two ROIs, one within the frontal (1a) and the other within the temporoparietal (2a) portion of the MCA territory, defined for comparison with the corresponding areas on the opposite side (1b, 2b). The automatically calculated relative values for CBF and CBV within the ROIs are shown in the table beneath the image. A = area of the ROI (in square centimeters), R = relative value compared with the corresponding area on the opposite side. Comparison of ROI 1a with the opposite side shows relative values of 61% and 77% for CBF and CBV, respectively. These values indicate oligemic tissue that is near the threshold for tissue at risk. The CBF and CBV values in area 2a are markedly to severely reduced, indicating brain tissue that will probably not survive. **(h, facing page)** Nonenhanced CT scan obtained 3 months after the onset of stroke demonstrates infarction of the left basal ganglia and temporoparietal MCA territory (arrows).

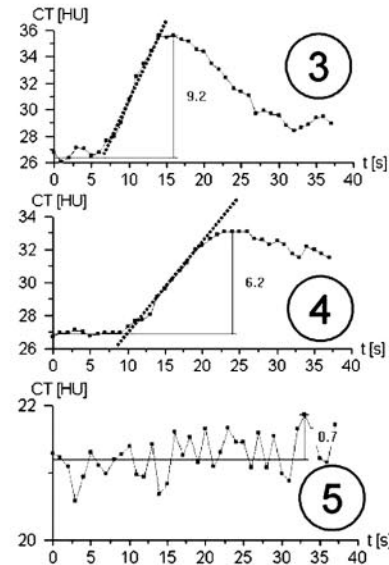


e.



| CBF | | | | |
|------|------|------|------|------|
| ROI: | 1a | 1b | 2a | 2b |
| A: | 5.3 | 5.1 | 6.9 | 6.7 |
| R: | 0.61 | 1.65 | 0.25 | 3.96 |
| CBV | | | | |
| A: | 5.3 | 5.1 | 6.9 | 6.7 |
| R: | 0.77 | 1.30 | 0.47 | 2.12 |

g.



f.



h.

Algorithm for Fast Interpretation of Perfusion CT Data within 3 Hours of Stroke Onset

| Pathologic Condition | Perfusion CT Finding | | |
|--|---------------------------------------|---------------------------|-----------------------------------|
| | TTP | CBF | CBV |
| None | Normal | Normal | Normal |
| Arterial stenosis or occlusion with excellent compensation | Prolonged | Normal | Normal |
| Oligemic tissue that will probably survive | Prolonged | Moderately reduced (>60%) | Normal or slightly reduced (>80%) |
| Tissue at risk | Prolonged | Markedly reduced (>30%) | Moderately reduced (>60%) |
| Tissue that is probably irreversibly damaged | Strong prolongation or not measurable | Severely reduced (<30%) | Severely reduced (<40%) |

Note.—Thresholds are valid only for the particular perfusion CT approach described in the article (30,35,39); they may vary for other approaches. Because various factors may influence outcome, the thresholds should not be used as absolute, singular classification values but rather as guidelines to aid in the interpretation of perfusion CT results.

Color-coded maps of these parameters are displayed for initial comparison of the cerebral hemispheres, allowing quick visual assessment of a possible infarction with a sensitivity of over 90% in larger ischemic lesions (35,38,39). The colors, which can be changed by manipulating window settings, should not be used to estimate the absolute values for CBF and CBV. When a unilateral ischemic lesion is suspected, the TACs for corresponding ROIs in the two hemispheres can be compared with dedicated graphical tools (Fig 3f), yielding the percentage of reduction of both CBF and CBV for the affected hemisphere versus CBF and CBV for the normal side.

TTP and MTT are very sensitive indicators of hemodynamic disturbances and should be evaluated at the beginning of the analysis of perfusion CT data. Both CBF and CBV help predict the outcome of an ischemic lesion. Reduced CBF with normal or even elevated CBV indicates that the autoregulation of the affected area is still functioning and that the tissue can possibly be revitalized or even survive without reperfusion. When both CBF and CBV are decreased, tissue at risk must be assumed. When both parameters are severely reduced or no longer measurable, irreversible damage has already occurred.

The Table shows a simplified algorithm for the interpretation (with use of the maximum slope model) of perfusion CT data in clinical practice. This algorithm is based on previous studies as well as our own experience (30,35,38,39). In a recent perfusion CT study that made use of the deconvolution model, a relative CBF threshold of 66% of the normal values of the normal hemisphere was determined to define an area that included infarction and tissue at risk on the affected side. An absolute threshold of 2.5 mL/100 g for CBV was used to define irreversibly damaged brain tissue (31).

The preliminary results of these studies will serve only as initial guidelines for the interpretation of perfusion CT data. Further studies involving a large number of patients are required to ascertain the reliability of these results and thresholds.

CT Angiography

CT angiography can be defined as a fast, thin-section, volumetric spiral CT examination performed with a time-optimized bolus of contrast material for the opacification of vessels (46). After the reformatting and inspection of cross-sectional images, 3D imaging is performed with a technique to be described later.

For a comprehensive diagnostic work-up in stroke patients, knowledge of the site of intracranial vessel occlusion and of possible stenosis,

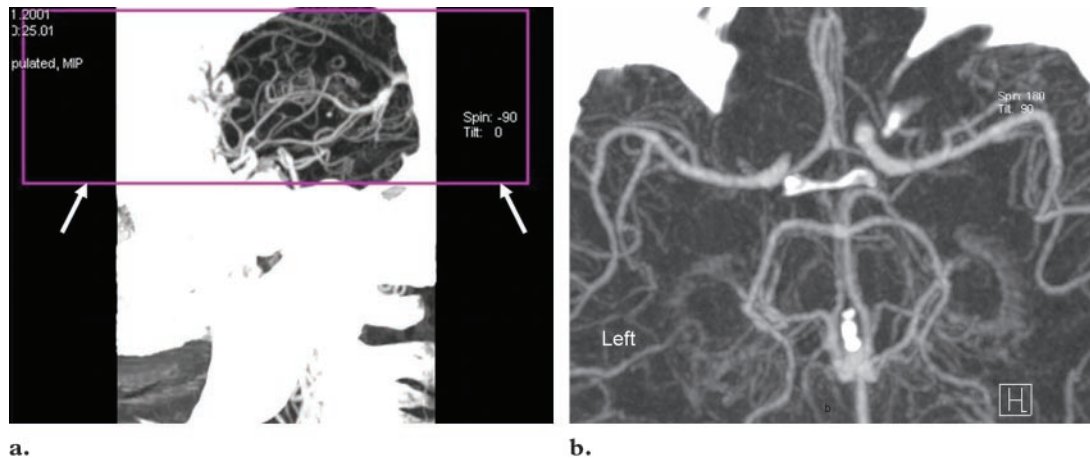


Figure 4. MIP imaging of the circle of Willis. A ROI is defined with use of a bounding box (arrows in **a**). Because the MIP algorithm demonstrates only the brightest voxels in a given volume, the skull base has been excluded. The resulting MIP image (superior view) is shown in **b**.

thrombosis, or occlusion of the carotid arteries as the underlying cause of the disease is essential. With modern multisection CT scanners, the entire region from the common carotid arteries up to the circle of Willis can be covered in a single data acquisition, with acquisition times under 20 seconds.

Data Acquisition.—To allow visualization of the vascular tree from the distal common carotid artery to the intracranial vessels, the examination includes the region from the fifth vertebral body up to the vertex. In our protocol, the following parameters were used: 120 kVp, 200 mAs, 4×1 -mm collimation, 5.5 mm/rotation table feed, and 0.5-second rotation time. We injected 100 mL of contrast material intravenously at a flow rate of 4 mL/sec with a power injector. For optimal timing of the bolus, the bolus tracking method (47) was used almost exclusively. After the start of contrast material injection, the software measures the attenuation values for a ROI within one of the common carotid arteries, and spiral scanning is automatically started as soon as the threshold of 100 HU is exceeded.

If bolus tracking is not available, the test bolus method should be applied for the timing of the data acquisition (48): Ten seconds after the bolus injection of 20 mL of contrast material, an axial single-section dynamic study (one scan every 2 seconds) is started below the level of the fifth cervical vertebral body and continues until the con-

trast material appears as hyperattenuating spots in the common carotid artery. With this technique, the time delay until the start of CT angiography can also be determined in individual cases.

The images were reformatted with a section thickness of 1.25 mm, an overlap of 0.7 mm, and a narrow field of view of 120 mm with high in-plane resolution, allowing high-quality 3D imaging.

Postprocessing and 3D Imaging.—To save time in the diagnostic work-up of acute ischemic stroke, all postprocessing procedures should be performed as quickly as possible. These procedures can be completed within 3 minutes with our protocol.

Occlusion or significant calcification of an internal carotid artery (ICA) can be detected immediately by surveying the source images on the workstation in combination with multiplanar reformatting. For the assessment of stenosis or occlusion of the MCA, which is difficult if made solely on the basis of source images, 3D imaging of the circle of Willis including both MCAs is needed (Fig 4). This 3D imaging is followed by imaging of the vertebral and basilar arteries, respectively (Fig 5), and finally by reformatting of images of the carotid arteries below the skull base (Figs 6, 7).

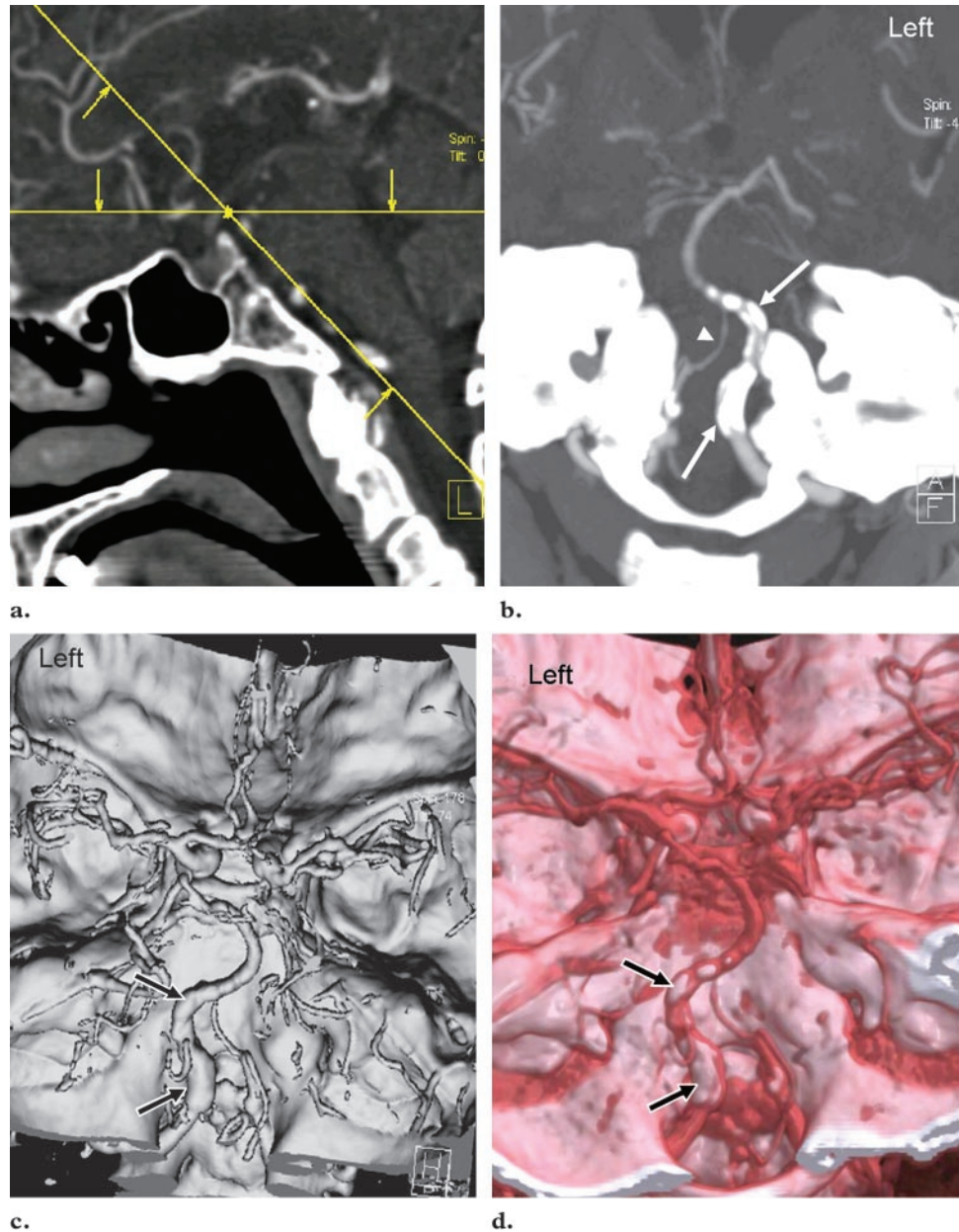
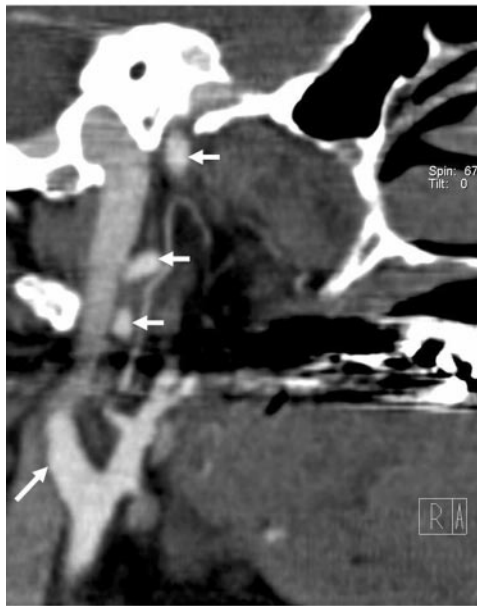


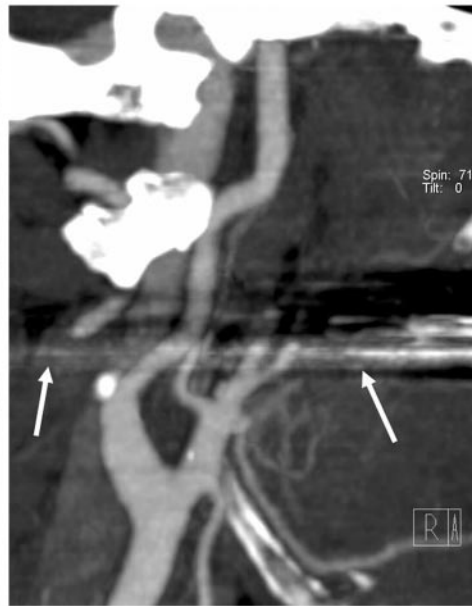
Figure 5. Three-dimensional imaging of the vertebral and basilar arteries from CT angiographic data. **(a)** On a sagittal multiplanar reformatted image obtained in the midline, a coronal plane is defined parallel to the clivus (diagonal yellow line). Horizontal yellow line indicates axial plane. **(b)** Anterior thin-section (10-mm) MIP image obtained in the coronal plane defined in **a** demonstrates the course of the distal vertebral arteries and the basilar artery. Note that in the area of calcification (arrows) it is impossible to see the lumen of the vessel. The right vertebral artery is hypoplastic (arrowhead). **(c)** Three-dimensional shaded surface display (SSD) image (upper posterior view) is not helpful in this case because it integrates the calcifications and the vessel wall, thereby giving the erroneous impression of enlarged rather than calcified arteries (arrows). **(d)** Three-dimensional volume-rendered (VR) image depicts the intracranial arteries and the calcifications within the vertebral and basilar arteries (arrows).



a.

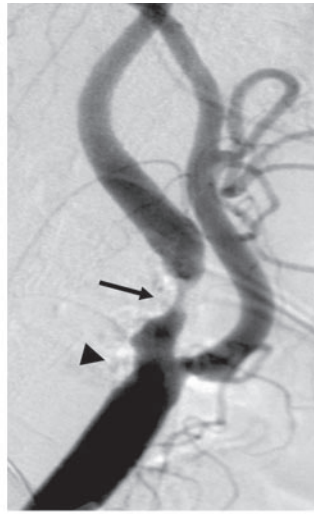


b.

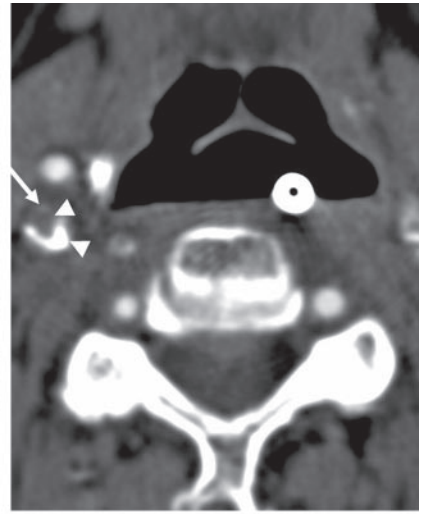


c.

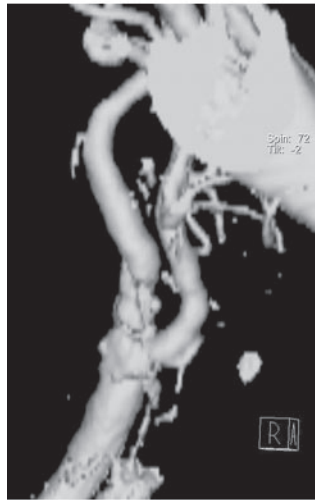
Figure 6. Fast analysis of the carotid bifurcation from CT angiographic data. **(a)** On an axial CT scan obtained a short distance above the bifurcation, a plane (arrows) is defined that will allow visualization of the right ICA. **(b)** Sagittal multiplanar reformatted image (right lateral view) obtained in the plane defined in **a** shows parts of the ICA from the bifurcation to the skull base (arrows). **(c)** Thin-section (15-mm) MIP image (right lateral view) obtained in the plane defined in **a** allows visualization of the entire length of the normal right ICA. Note the moderate artifacts due to dental inlays (arrows).



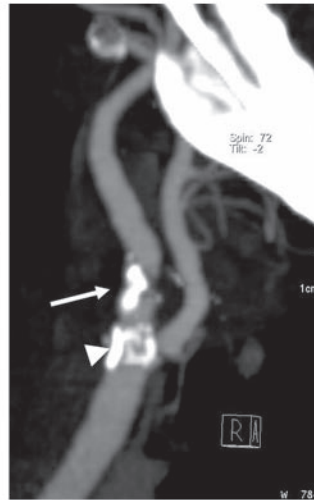
a.



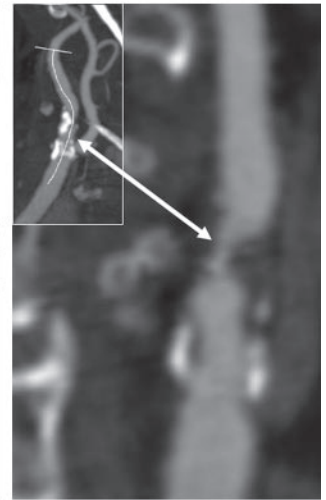
b.



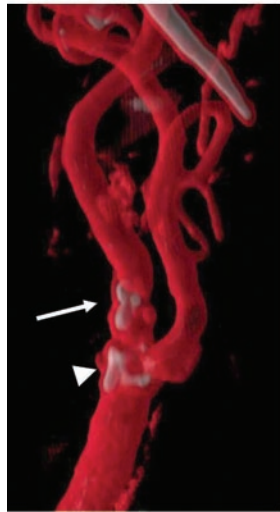
c.



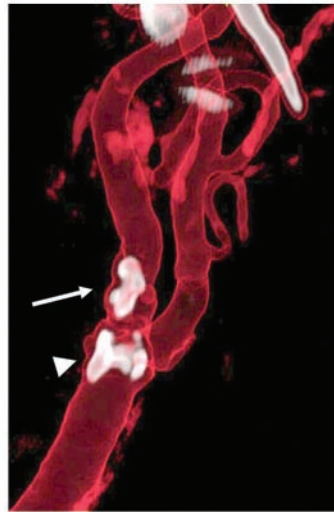
d.



e.



f.



g.



h.

Figure 7. Evaluation of the right carotid bifurcation from CT angiographic data with use of right lateral 3D images. **(a)** Digital subtraction angiogram clearly demonstrates the extent of a primary calcified stenosis (arrow). A second minor calcified stenosis is also seen (arrowhead). **(b)** Axial CT scan shows severe stenosis of the right ICA. The blood-filled lumen within the stenosis is visible as a small white spot (arrow). A surrounding soft plaque (top arrowhead) and calcifications (bottom arrowhead) are also seen. **(c)** On an SSD image, the stenosis is not visible because the calcifications cannot be differentiated from the lumen of the artery. **(d)** MIP image shows the calcified stenosis (arrow), but the degree of stenosis is difficult to determine. In addition, it is hard to say whether the inferior calcification (arrowhead) narrows the lumen of the carotid artery. **(e)** Curved multiplanar reformatted image obtained in the area of the stenosis allows better estimation of the degree of stenosis than does the MIP image (inset). Double-headed arrow indicates corresponding anatomic structures on the two images. **(f)** High-opacity VR image shows the carotid bifurcation and allows visualization of both the superior (arrow) and inferior (arrowhead) calcifications. **(g, h)** Lower-opacity VR images allow estimation of the degree of stenosis (arrow). The inferior calcification (arrowhead) is better visualized with a more superior view **(h)**, which demonstrates that the circumferential plaque (cf **b**) does not cause significant stenosis.

Knowledge of the basic principles of common methods of 3D imaging is necessary to ensure extraction of the optimal spatial information about vascular structures from the volume data without eliminating important anatomic structures. There are currently no standards for the orientation of 3D reformatted images of intracranial vessels. In this article, a superior view is used for the circle of Willis, a right lateral view for the right carotid bifurcation, and a left lateral view for the left carotid bifurcation.

At present, three methods of 3D imaging are used (49):

1. Maximum intensity projection. MIP is still the most commonly used method because it is part of the standard postprocessing software of modern CT scanners and MR imagers. This technique causes significant loss of information because only the single layer of the brightest voxels in a given plane is displayed (50). Therefore, the “attenuation” information (which, for example, helps differentiate between contrast material-filled arteries and calcifications) is preserved, whereas the “depth” information (which helps determine which anatomic structures are “closer” and which are “farther away”) is completely lost. MIP is useful for rapid detection of vascular discontinuities but may fail to accurately depict important findings like stenosis due to distinct overlying calcifications (Figs 5b, 7d). The hyperattenuating skull, which impedes the view of the lower-attenuation intracranial vessels, must be “removed” manually (Fig 4). In patients with MCAs that are close to the skull base, care must be taken not to eliminate parts of the vessels together with the adjacent bone, which may lead to misdiagnosis as an MCA occlusion.

2. Shaded surface display. With SSD, the first layer of voxels within defined thresholds (in Hounsfield units) is used for display, leading to the visualization of the surface of all structures (eg, intracranial vessels) that fulfill the threshold conditions. Unlike with MIP, the “depth” information is preserved but the “attenuation” information is lost with SSD. Arteries will appear to vary in caliber depending on the thresholds that are selected, and a middle-grade stenosis might easily be misinterpreted as an occlusion (51). Calcifications that cannot be differentiated from the vessel wall might give the erroneous impression of dilatation, even in cases of severe stenosis (Figs 5c, 7c).

3. Volume rendering. VR principally allows the integration of all available information from a volumetric data set (49,52–54). Groups of voxels within defined attenuation thresholds are selected, and a color as well as an “opacity” is assigned. A low opacity leads to transparent images and vice versa. Unlike MIP and SSD images, VR images are created, not from a single layer of voxels, but from all voxels that meet the selection criteria. With this technique, it is possible to demonstrate (for example) a calcified ICA (Fig 7f–7h) or the circle of Willis together with the skull base in different colors (Fig 5d). Therefore, if available, VR is the best choice for 3D imaging of extra- and intracranial vessels.

Because all methods of 3D imaging are subject to some loss of information, none of them can substitute for the thorough analysis of source images.

For quick initial evaluation of the vascular situation, our stroke protocol comprises the following multiplanar reformatting and MIP techniques:

1. The source images are inspected first to detect occluded arteries, thrombosis, and major calcifications.

2. MIP images of the circle of Willis are created as shown in Figure 4.

3. Multiplanar reformatting and thin (10–20-mm) MIP images are used to quickly visualize the basilar artery (Fig 5a, 5b) and the carotid arteries (Fig 6).

4. If calcifications of the vessel wall are present, the degree of stenosis can be assessed with source images or curved multiplanar reformatted images (Fig 7b, 7e).

Image Interpretation.—Data analysis must start with the inspection of the source images, preferably on a workstation that allows multiplanar reformatting. Thus, occlusion of an ICA and calcified stenosis or thrombosis of major arteries can often be easily detected by comparing the corresponding arteries in the two hemispheres. In patients with a suspected MCA occlusion, the next step is 3D imaging of the circle of Willis. When MIP is used, vessel occlusion is easily detected after removal of the skull base (Figs 4b, 5b).

SSD and VR do not require removal of the skull base (Fig 5c, 5d). Because these methods are threshold based, an MCA stenosis or occlusion can be evaluated by decreasing the lower threshold with corresponding growth in the diameter of the artery until noise from the surrounding tissue appears. SSD, which cannot help differentiate between calcifications and contrast-enhanced arteries, should be applied only after inspection of the source images or MIP images.

In patients with suspected ICA disease, occlusion of one ICA is easily identified due to lack of

contrast enhancement compared with the normal contralateral ICA. As long as there are no calcifications, the carotid bifurcation can be sufficiently visualized with MIP images to allow initial analysis (Fig 6c). When calcifications obscure a stenosis (Fig 7d), axial source images or curved multiplanar reformatted images are most helpful in evaluating the stenosis (55). For reasons mentioned earlier, SSD is not helpful in arteries with calcified stenosis (51), whereas VR can produce reasonably high-quality images in addition to cross-sectional images and curved multiplanar reformatted images in selected cases (56).

CT angiography of the carotid bifurcation may be disturbed by beam-hardening artifacts from dental fillings (Fig 6c). However, in our series, evaluation of carotid stenosis was impossible due to dental artifacts in only two of 85 patients. In the remaining 83 patients, the resulting images were of good or at least reasonably good quality.

Comprehensive Imaging of Ischemic Stroke with Multisection CT

At present, there is insufficient scientific evidence to speak of an optimal therapy for the various patterns of findings in stroke patients. All randomized studies of thrombolysis in acute stroke have been based on nonenhanced CT findings alone without further information concerning possible vascular stenosis or changes in brain perfusion.

With the new imaging modalities of perfusion CT and CT angiography, stroke patients can now be evaluated more precisely and consequently treated according to their individual needs, thus avoiding the potential harm of performing thrombolysis in patients with (a) a large amount of irreversibly damaged brain tissue or (b) reversible cerebral ischemia, in which spontaneous reperfusion of ischemic tissue may occur (57). The combined application of multisection CT techniques in our series of patients with acute stroke revealed different typical combinations of findings.

In patients with clinical symptoms of ischemic stroke but no pathologic findings at any of the

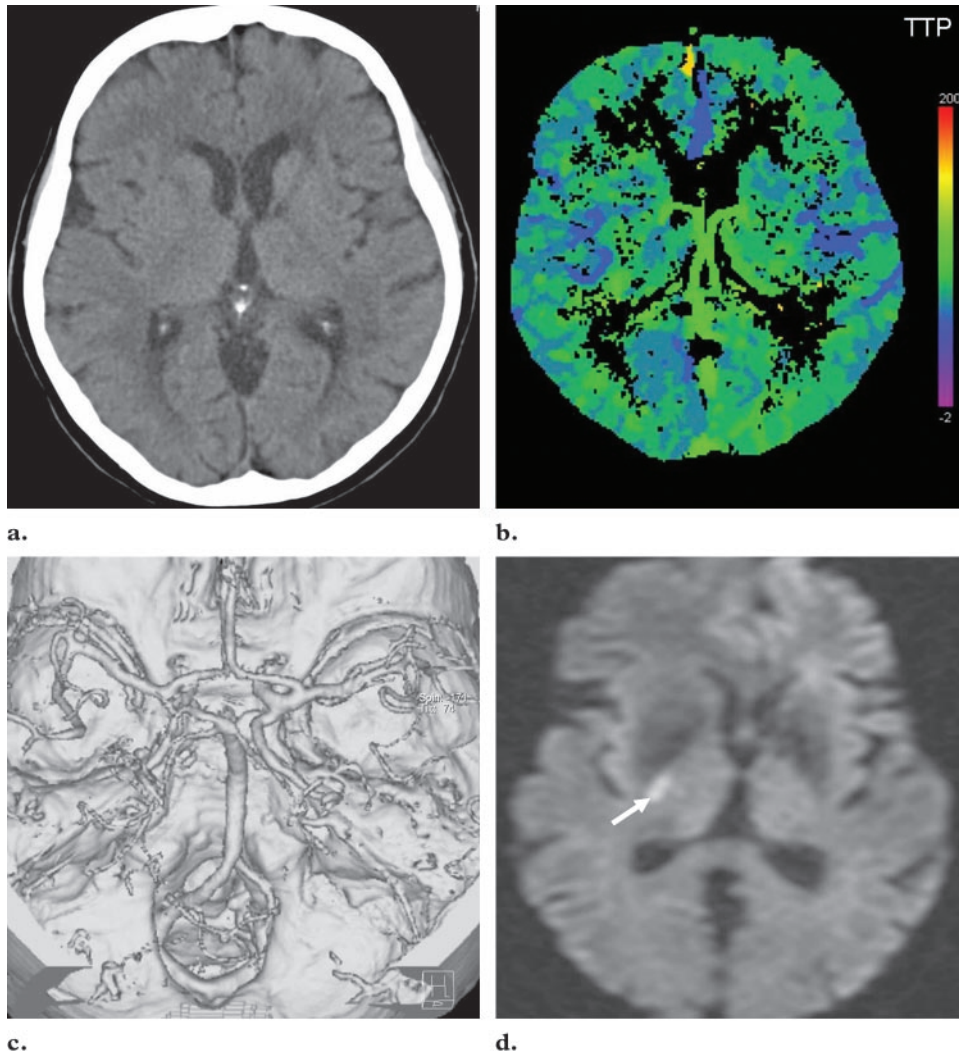
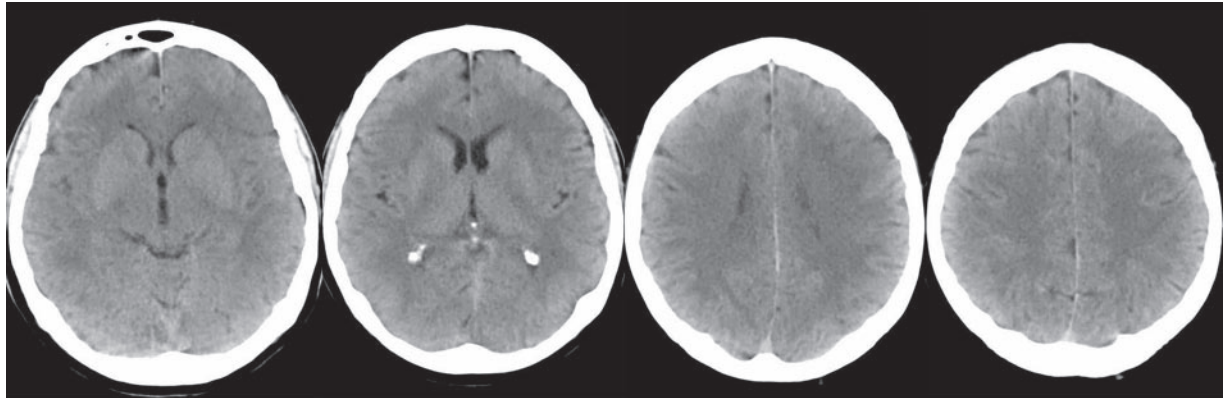


Figure 8. (a–c) Nonenhanced CT scan (a), perfusion CT scan (b), and SSD image from CT angiography (c) obtained 2 hours after the onset of symptoms in a 65-year-old woman with left hemiplegia demonstrate normal findings. (d) Diffusion-weighted MR image ($b = 1,000 \text{ s/mm}^2$) shows a small ischemic lesion in the right posterior internal capsule (arrow).

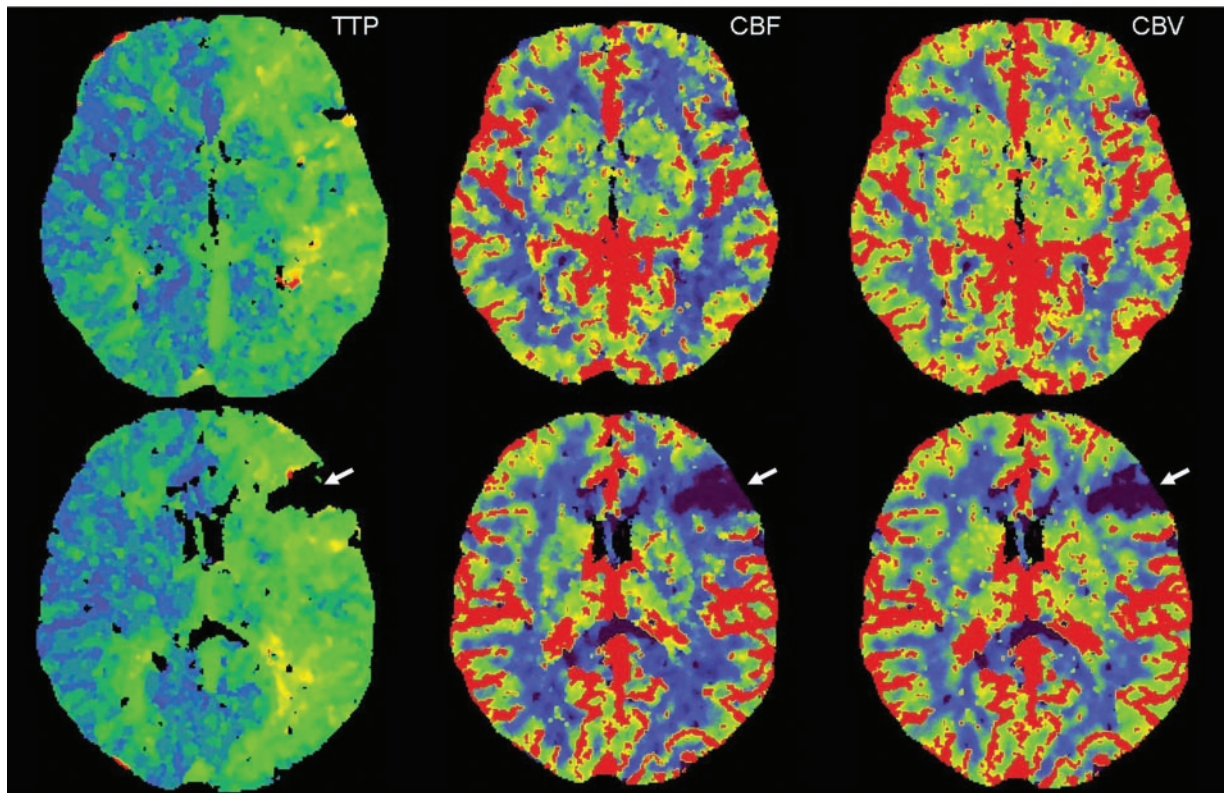
three studies, a large MCA infarction can be excluded. This information is sufficient for the therapeutic decision not to perform thrombolysis, although smaller ischemic lesions outside the 2–3-cm section covered by perfusion CT may be missed (58). The latter shortcoming represents a

clear disadvantage relative to MR imaging (including diffusion-weighted imaging), with which even very small ischemic lesions can be detected (Fig 8).

Figure 9. (a) Nonenhanced CT scans obtained 5 hours after the onset of symptoms in a 60-year-old man with motoric aphasia and slight right hemiparesis demonstrate normal findings. (b) Perfusion CT study shows a small, wedge-shaped area of nonperfused brain in the left frontal lobe that is best seen on the lower images (arrow). In addition, there is a 3-second prolongation of TTP (measurement not shown) within the entire left hemisphere (green area on TTP maps). (*Fig 9 continues.*)

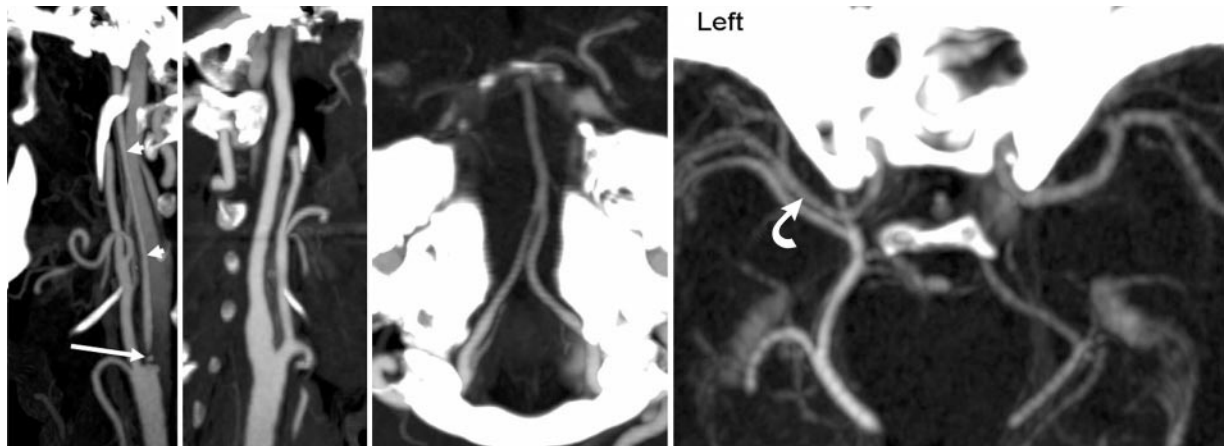


a.

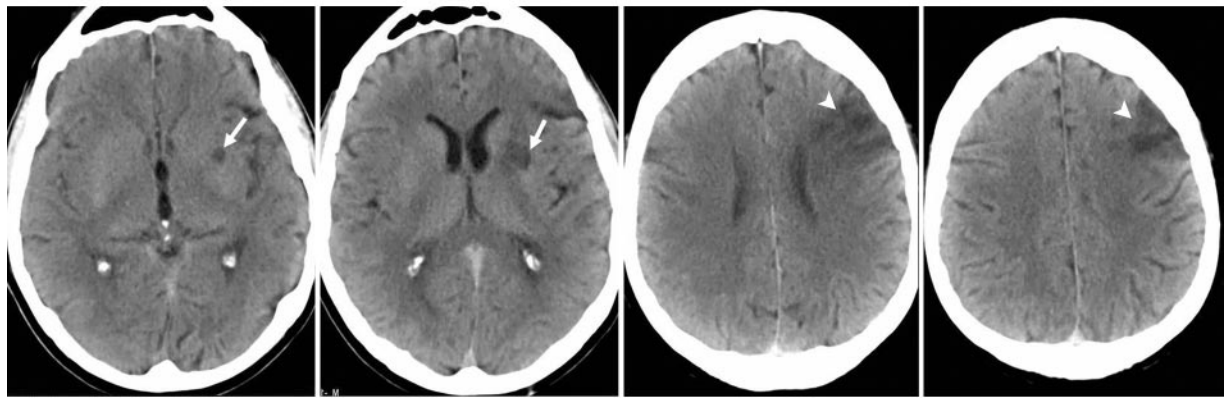


b.

Figure 9 (continued). (c) MIP images from CT angiography show a high-grade stenosis of the left ICA (straight arrow) that results in narrowing of the distal lumen of the ICA (arrowheads) and of the MCA (curved arrow). The right carotid artery and the basilar artery are normal. (d) Nonenhanced CT scans obtained 3 weeks after the onset of stroke demonstrate infarction of the frontal portion of the lentiform nucleus (arrow) and a small infarction in the left frontal lobe (arrowhead).



c.



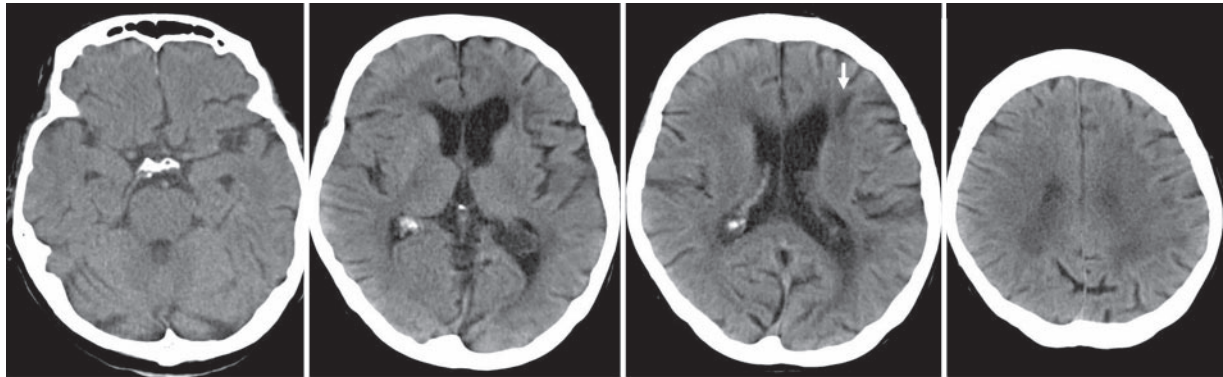
d.

In the rather common constellation that consists of high-grade ICA stenosis and a patent MCA with no or only minor ischemia within the MCA territory (Fig 9), perfusion CT typically shows prolongation of TTP (or MTT) together with normal CBF and CBV values as long as the autoregulation compensates for the delayed arrival of the contrast material. In these cases, small infarctions may be more easily missed with single-section perfusion CT than with multisection perfusion CT, which covers a higher percentage of the MCA territory (Fig 9b). Curved multiplanar

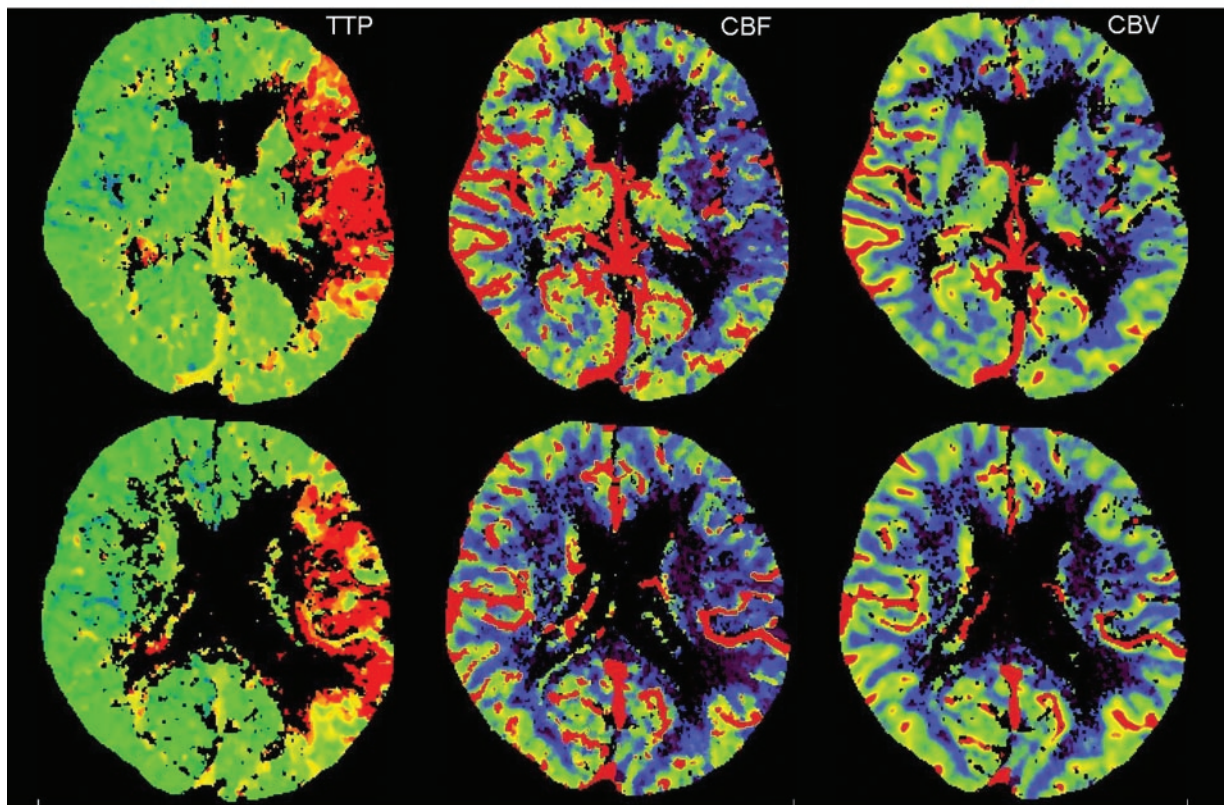
reformatting and VR are better suited for a more detailed analysis of stenosis of the ICA. If the ICA stenosis in the aforementioned constellation is symptomatic for hemodynamic reasons, patients should not undergo thrombolysis.

Another constellation of findings includes normal findings or subtle early signs at nonenhanced CT, tissue at risk at perfusion CT, and MCA occlusion at CT angiography. This most challenging situation with respect to selection of patients

Figure 10. (a) Nonenhanced CT scans obtained 35 minutes after the onset of symptoms in a 76-year-old woman with complete aphasia and right hemiplegia demonstrate an old ischemic lesion in the left frontal lobe (arrow) but no early signs of infarction. (b) Perfusion CT study demonstrates a large region of markedly reduced perfusion (red area on the TTP maps, blue area on the CBF and CBV maps). Comparison with the opposite hemisphere yielded relative values of 43% and 63% for CBF and CBV, respectively, findings that indicate tissue at risk. The patient's symptoms resolved spontaneously 30 minutes after the CT examination. (*Fig 10 continues.*)



a.

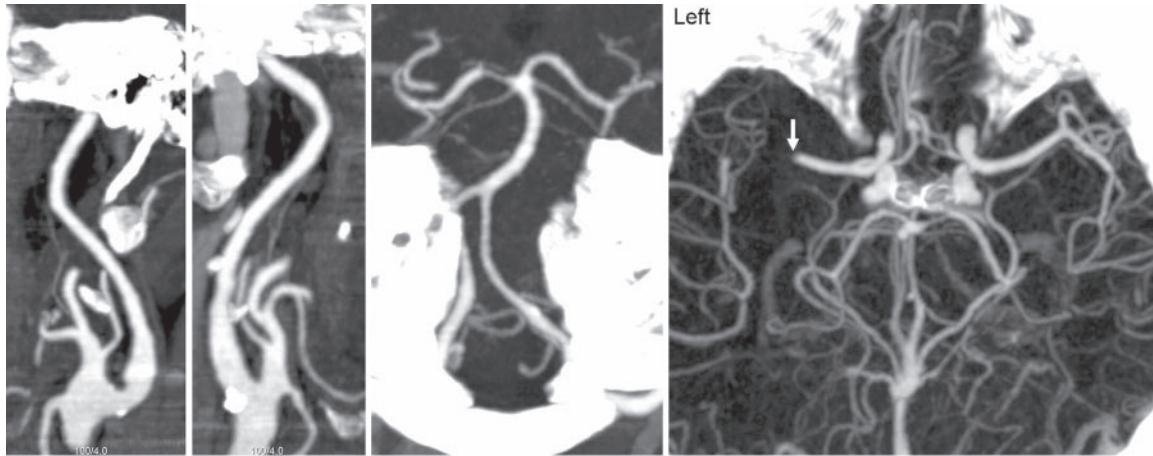


b.

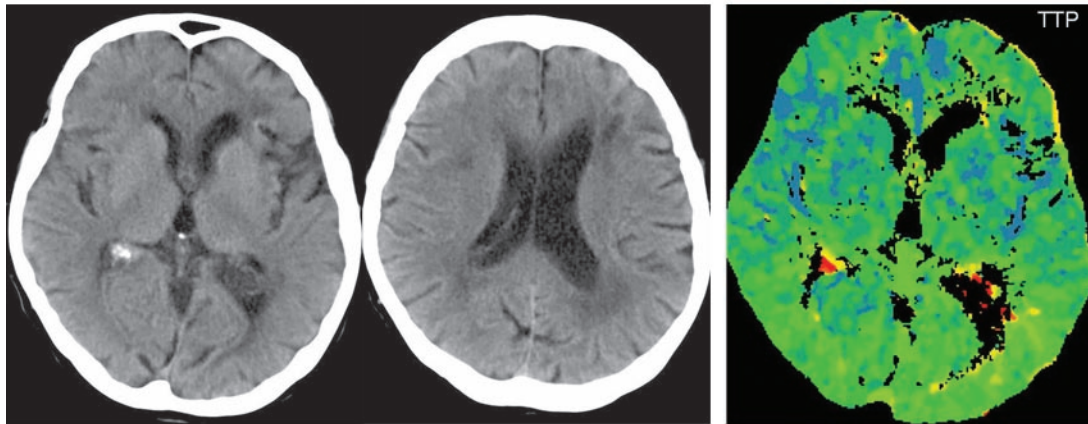
for thrombolysis is illustrated in Figures 10 and 11. In the very early stage, nonenhanced CT will demonstrate no or only minor early signs of infarction (Fig 11a). Perfusion CT can more reli-

ably help identify irreversibly damaged brain tissue and allows estimation of the extent of tissue at risk within the investigated area (Figs 10b, 11b). The site of the MCA occlusion is visualized simultaneously at CT angiography (Figs 10c, 11c).

Figure 10 (continued). (c) MIP images (superior view) from CT angiography show occlusion of the left MCA (arrow). The carotid arteries and the basilar artery are normal. (d) Nonenhanced CT scans obtained 24 hours after the onset of stroke do not show any changes from the initial examination (cf a). (e) Follow-up perfusion CT scan shows a normal color map of TTP with symmetric perfusion. (f) CT angiogram demonstrates spontaneous recanalization of the MCA.

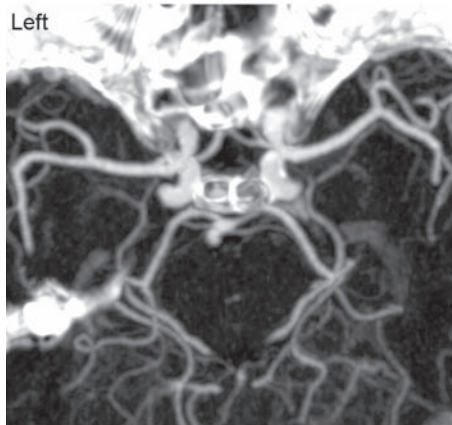


c.



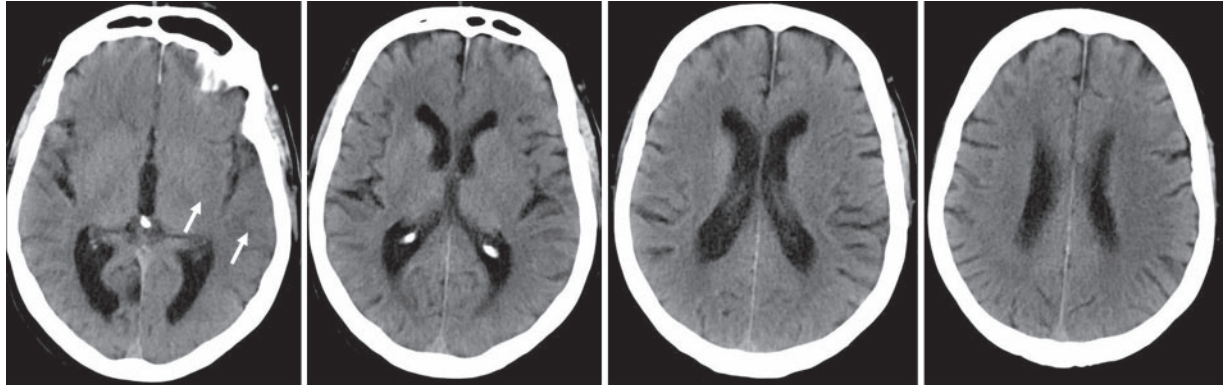
d.

e.

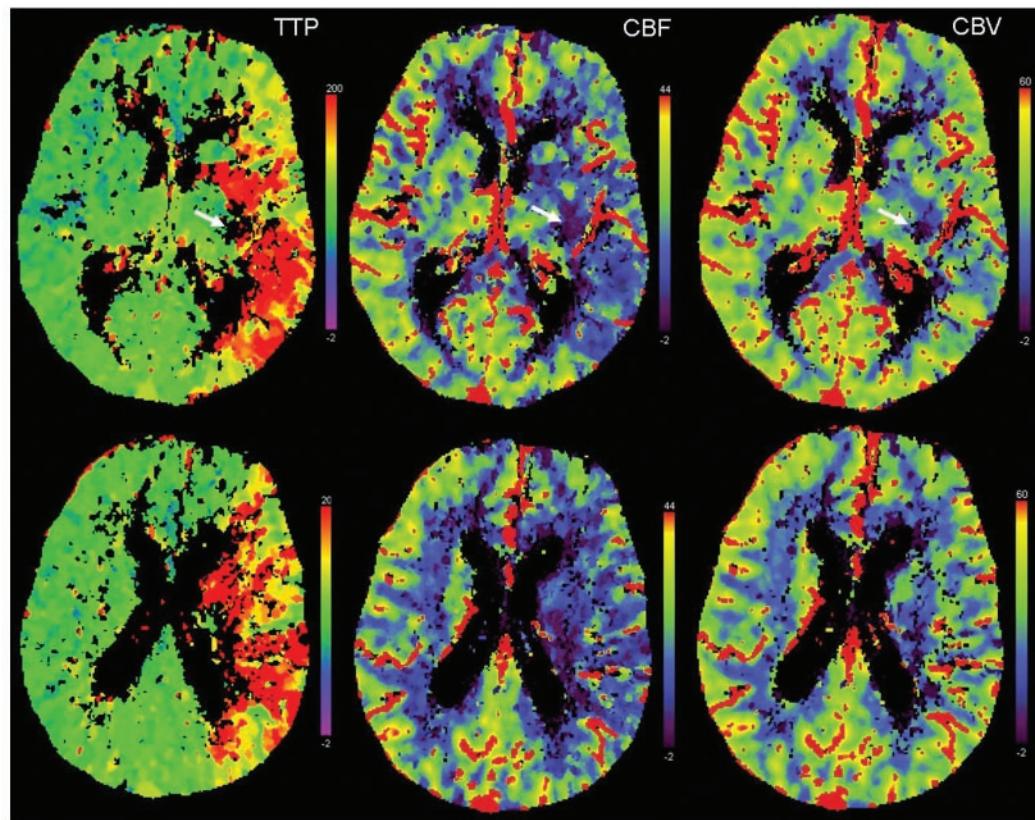


f.

Figure 11. (a) Nonenhanced CT scans obtained 2½ hours after the onset of symptoms in a 73-year-old man with right hemiplegia and complete aphasia demonstrate partial obscuration of the lentiform nucleus and subtle swelling and hypoattenuation of the left temporal lobe (arrows), findings that indicate infarction. (b) Perfusion CT study demonstrates relative values of 60% and 72% for CBF and CBV, respectively within the MCA territory, findings that indicate tissue at risk. In addition, a small area of nonperfusion is seen within the lentiform nucleus (arrow). (*Fig 11 continues.*)



a.

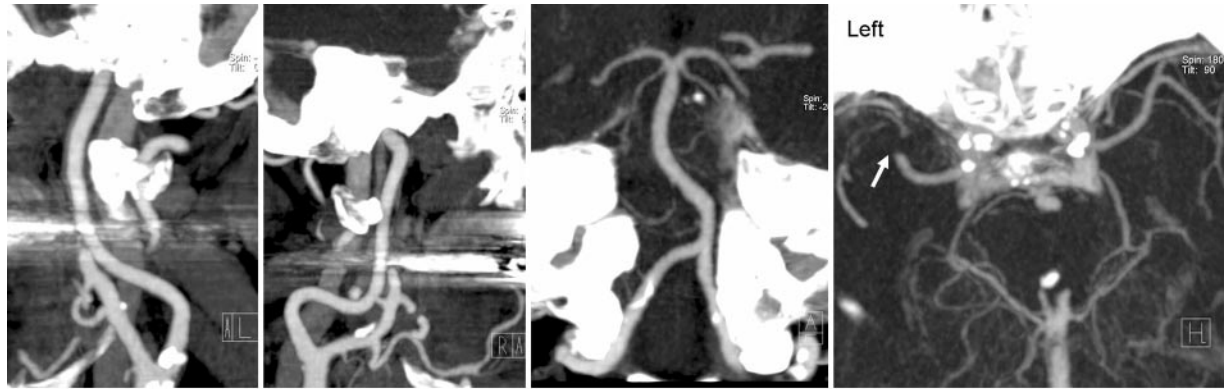


b.

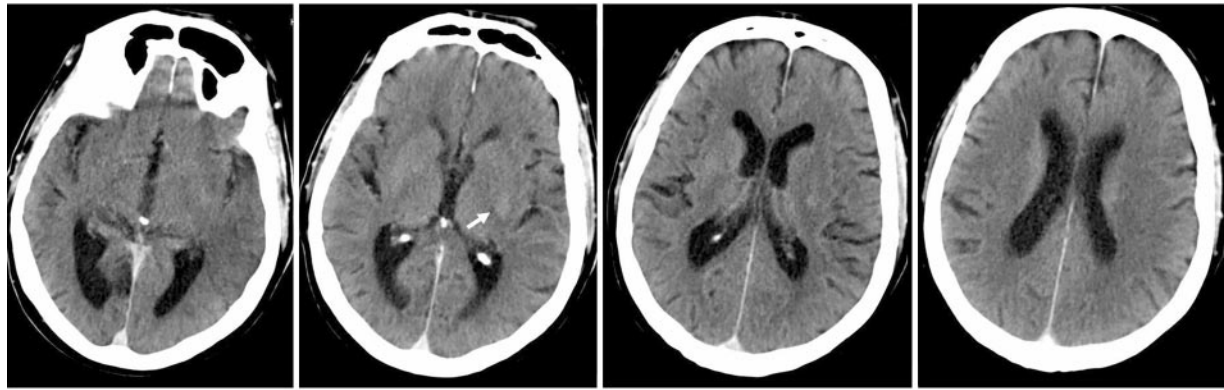
At present, no reliable data exist that indicate how long ischemic brain tissue can survive after the acute event before being revitalized with recanalization. Animal studies published by Jones et al in 1981 (27) showed that the chances of af-

ected tissue being revitalized with recanalization decrease over time. Currently, a therapeutic window of 3 hours is accepted for safe and effective thrombolysis in patients with ischemic stroke (6). This narrow window can probably be expanded to 6 hours or more in selected patients as long as neuroimaging with multimodal multisection CT

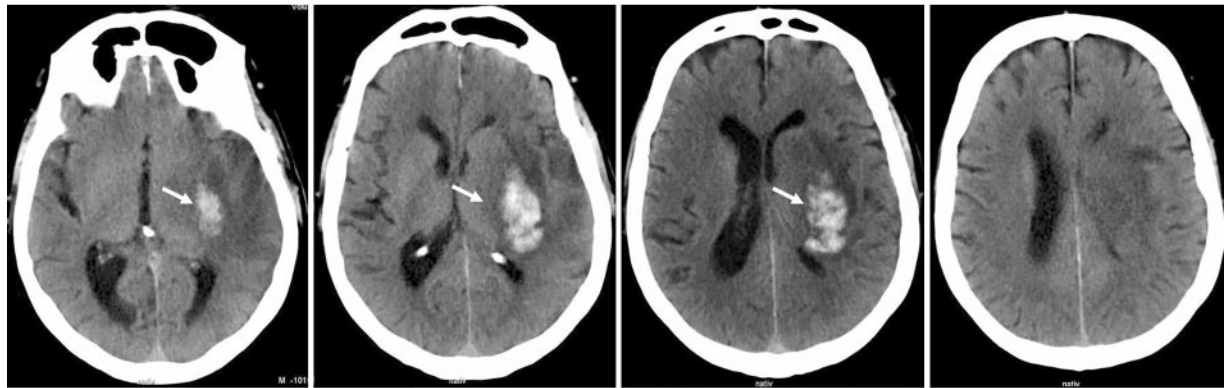
Figure 11 (continued). (c) MIP images (superior view) from CT angiography show distal occlusion of the left MCA (arrow). The carotid arteries and basilar artery are normal except for calcification of the left carotid bifurcation (far left). (d) Nonenhanced CT scans obtained 2 hours after the onset of systemic intravenous thrombolysis show the beginning of hemorrhagic transformation of the lentiform nucleus (arrow) and increasing hypoattenuation within the temporal lobe. Follow-up CT angiography demonstrated patency of the MCA, a finding that indicated successful thrombolysis. (e) CT scans obtained 2 days later show that the hemorrhage has increased in size (arrow). There is no infarction in the cortex of the MCA territory except in the temporal lobe.



c.



d.

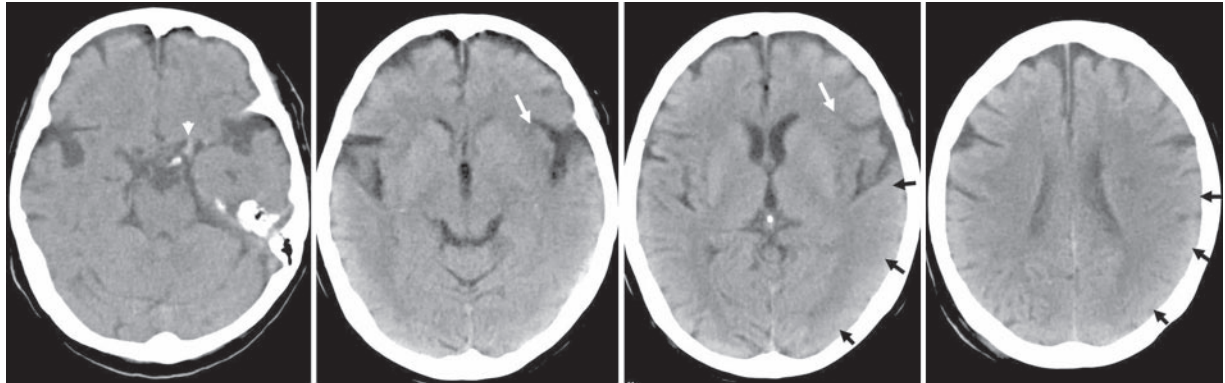


e.

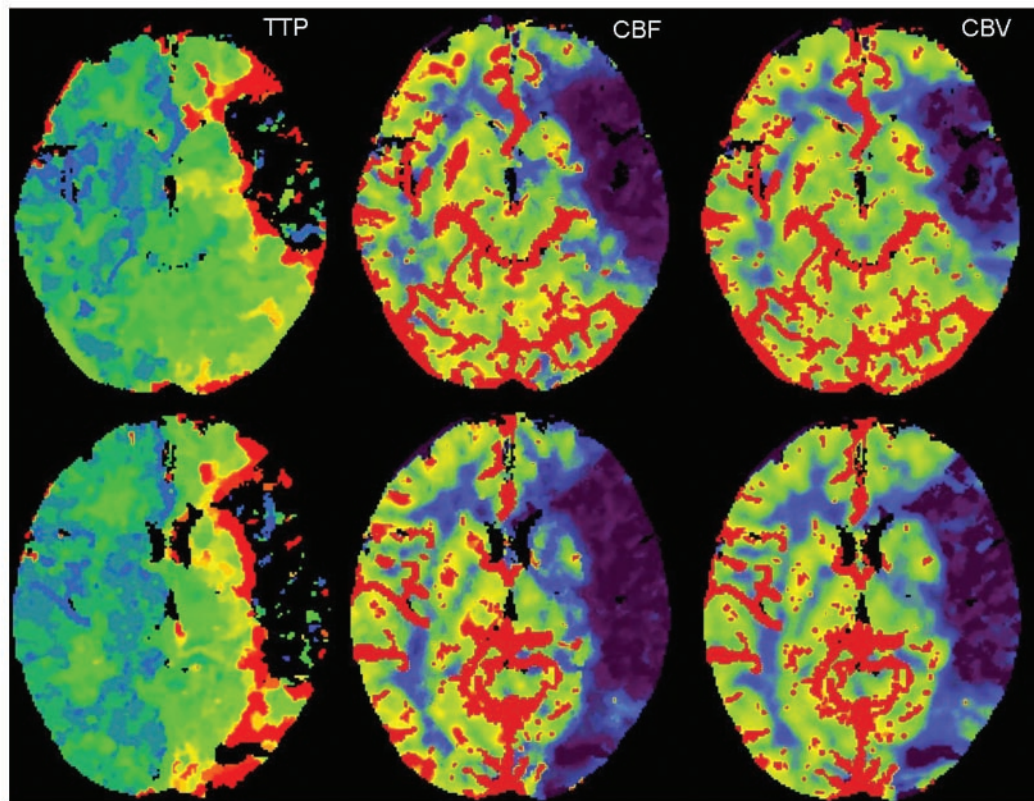
or MR imaging shows a larger area of tissue at risk that can still be saved (59). In cases of a gradual build-up of arterial occlusion involving a growing number of branches, the time window might be different for different areas of the tissue at risk. Modern neuroimaging helps evaluate the

dynamic process of ischemic stroke, thereby aiding in the selection of the appropriate therapy for patients with various stages of ischemia without the use of preset therapeutic windows.

Figure 12. (a) Initial nonenhanced CT scans obtained 3 hours after the onset of stroke in a 77-year-old woman show effacement of the sulci in the area of the left MCA territory (black arrows) as well as “loss” of the insular ribbon (white arrow) and a hyperattenuating proximal MCA (arrowhead). (b) Perfusion CT study shows nonperfusion of the left MCA territory. On the TTP maps, the residual parts of the left hemisphere have a different color than the right hemisphere, a finding that indicates slight prolongation of TTP, which was calculated at about 1 second. (*Fig 12 continues.*)

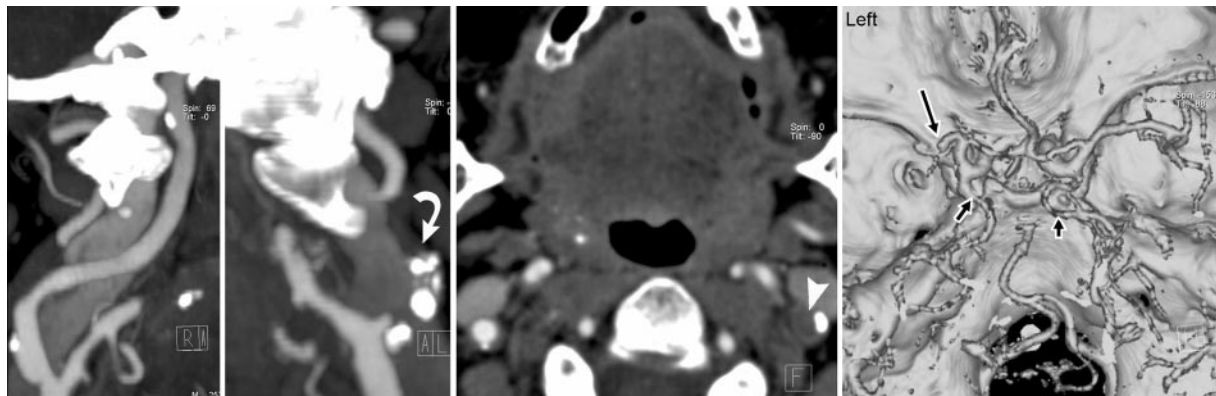


a.

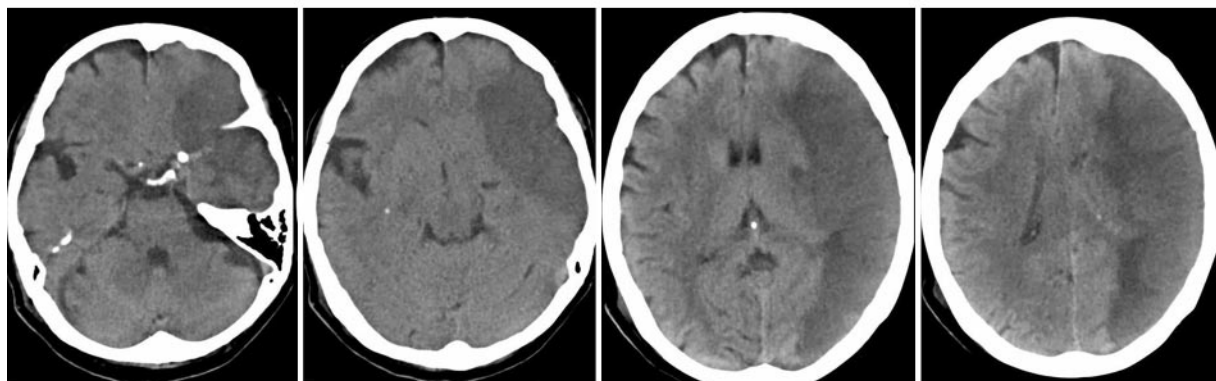


b.

Figure 12 (continued). (c) MIP images (left frontolateral view) and an SSD image (superior view) (far right) from CT angiography show proximal occlusion of the left MCA (white arrow) as well as occlusion of the left ICA (arrowhead). Note that the posterior cerebral arteries are predominantly supplied by the posterior communicating arteries (black arrows). This is a common anatomic variant and explains why the subtle TTP prolongation includes the territory of the posterior cerebral artery. (d) Nonenhanced CT scans obtained 1 day later show hypoattenuating swelling in the left MCA territory.



c.



d.

Nevertheless, the therapeutic decision remains problematic in many patients (Figs 10, 11). Figure 10 was obtained in a patient with occlusion of the left MCA. The patient recovered shortly after the examination without undergoing therapy, probably due to rapid autolysis of the thrombus. Application of a thrombolytic agent would have led to a false-positive treatment result.

Figure 11 was obtained in a patient who underwent thrombolysis despite the already present early signs (eg, hypoattenuation of the temporal portion [clearly less than one-third] of the MCA territory and of the lentiform nucleus). The procedure allowed the tissue at risk to be saved but caused severe intracranial hemorrhage into the

basal ganglia, leaving the patient with permanent hemiplegia.

In other cases of ischemic stroke, findings include normal findings or early signs at nonenhanced CT, nonperfusion of the MCA territory at perfusion CT, and MCA occlusion at CT angiography. Within 3 hours after the onset of a major stroke, when assessment of the full extent of irreversible ischemic damage may not yet be possible solely on the basis of early signs, perfusion CT allows reliable delineation of the area of irreversibly damaged brain tissue within the affected vascular territory (Fig 12) (30,31,35,39,60). When

the proximal portion of the MCA is occluded, the basal ganglia are also affected, whereas in cases of occlusion distal to the lenticulostriate end-branches, the basal ganglia will be preserved. Large studies investigating the usefulness of perfusion CT in making the therapeutic decision whether to perform thrombolysis in individual cases are not yet available. Preliminary experience suggests that in patients with complete loss of perfusion of the MCA territory on perfusion CT scans, thrombolytic therapy will be harmful rather than helpful.

Multisection CT Versus Other Imaging Modalities

A detailed investigation of cerebral perfusion might also include positron emission tomography (PET), single-photon emission computed tomography (SPECT), and xenon CT. However, the availability of these modalities is often limited, and their use can be problematic in an emergency situation in which “time is brain” (57). In recent years, multimodal MR imaging including diffusion- and perfusion-weighted imaging has been used successfully in the evaluation of infarction and tissue at risk (61–64). The examination can be completed within 30 minutes in an optimized setting (65). However, multisection CT scanners are more readily available than MR imagers in most radiology departments, and treatment of uncooperative patients in the initial stage of acute stroke is often more difficult in an MR imager. The main disadvantage of multisection perfusion CT is its limitation to a 2–3-cm section of brain tissue, so that ischemic lesions beyond this range are missed. The following alternatives may help solve this problem:

1. Investigating more than one region, albeit at the expense of increased doses of contrast material and radiation (39,66).

2. Moving the CT table during dynamic scanning (“toggling table” method) (67). However, so far this method is available only on an experimental basis and most likely will not provide adequate temporal resolution for optimal acquisition of dynamic scans.

3. Carefully inspecting the CT angiography source images, which enables prediction of the extent of an infarction by allowing detection of nonenhanced areas (68).

In a recent comparative study, Wintermark et al (66) showed that perfusion CT and MR imaging (including diffusion-weighted imaging and perfusion MR imaging) are equally valuable in the assessment of tissue at risk in patients with clinical symptoms related to ischemia of the MCA territory.

Conclusions

Multimodal multisection CT can rapidly provide comprehensive information regarding the extent of ischemic damage in acute stroke patients. Prospective studies involving a large number of patients will be needed to ascertain the treatment of choice for the various patterns of findings in ischemic stroke, which can now be analyzed more clearly with the combined use of multisection CT and MR imaging.

References

1. Tissue plasminogen activator for acute ischemic stroke. The National Institute of Neurological Disorders and Stroke rt-PA Stroke Study Group. *N Engl J Med* 1995; 333:1581–1587.
2. Beauchamp NJ Jr, Barker PB, Wang PY, vanZijl PC. Imaging of acute cerebral ischemia. *Radiology* 1999; 212:307–324.
3. Wardlaw JM. Overview of Cochrane thrombolysis meta-analysis. *Neurology* 2001; 57:S69–S76.
4. Prokop M. Multislice CT angiography. *Eur J Radiol* 2000; 36:86–96.
5. Hacke W, Brodt T, Caplan L, et al. Thrombolysis in acute ischemic stroke: controlled trials and clinical experience. *Neurology* 1999; 53:S3–S14.
6. Kaste M, Thomassen L, Grund M, et al. Thrombolysis for acute ischemic stroke: a consensus statement of the 3rd Karolinska Stroke Update, October 30–31, 2000. *Stroke* 2001; 32:2717–2718.
7. Astrup J, Siesjo BK, Symon L. Thresholds in cerebral ischemia: the ischemic penumbra. *Stroke* 1981; 12:723–725.
8. Hakim AM. Ischemic penumbra: the therapeutic window. *Neurology* 1998; 51:S44–S46.
9. von Kummer R. Effect of training in reading CT scans on patient selection for ECASS II. *Neurology* 1998; 51:S50–S52.
10. Kalafut MA, Schriger DL, Saver JL, Starkman S. Detection of early CT signs of >1/3 middle cerebral artery infarctions: interrater reliability and sensitivity of CT interpretation by physicians involved in acute stroke care. *Stroke* 2000; 31:1667–1671.
11. Rydberg J, Buckwalter KA, Caldemeyer KS, et al. Multisection CT: scanning techniques and clinical applications. *RadioGraphics* 2000; 20:1787–1806.
12. Ros PR, Ji H. Special Focus Session: multisection (multidetector) CT—applications in the abdomen. *RadioGraphics* 2002; 22:697–700.
13. Lell M, Wildberger JE, Heuschmid M, et al. CT-angiography of the carotid artery: first results with a novel 16-slice-spiral-CT scanner. *Rofo Fortschr Geb Rontgenstr Neuen Bildgeb Verfahr* 2002; 174:1165–1169. [German]
14. Tomura N, Uemura K, Inugami A, Fujita H, Higano S, Shishido F. Early CT finding in cerebral infarction: obscuration of the lentiform nucleus. *Radiology* 1988; 168:463–467.
15. Truwit CL, Barkovich AJ, Gean-Marton A, Hibri N, Norman D. Loss of the insular ribbon: another early CT sign of acute middle cerebral artery infarction. *Radiology* 1990; 176:801–806.
16. Schuierer G, Huk W. The unilateral hyperdense middle cerebral artery: an early CT-sign of embolism or thrombosis. *Neuroradiology* 1988; 30:120–122.

17. Manelfe C, Larrue V, von Kummer R, et al. Association of hyperdense middle cerebral artery sign with clinical outcome in patients treated with tissue plasminogen activator. *Stroke* 1999; 30:769–772.
18. Tomsick T, Brott T, Barsan W, et al. Prognostic value of the hyperdense middle cerebral artery sign and stroke scale score before ultraearly thrombolytic therapy. *AJNR Am J Neuroradiol* 1996; 17:79–85.
19. Leys D, Pruvo JP, Godefroy O, Rondepierre P, Leclerc X. Prevalence and significance of hyperdense middle cerebral artery in acute stroke. *Stroke* 1992; 23:317–324.
20. Barber PA, Demchuk AM, Hudon ME, Pexman JH, Hill MD, Buchan AM. Hyperdense sylvian fissure MCA “dot” sign: a CT marker of acute ischemia. *Stroke* 2001; 32:84–88.
21. von Kummer R, Bourquain H, Bastianello S, et al. Early prediction of irreversible brain damage after ischemic stroke at CT. *Radiology* 2001; 219:95–100.
22. Grotta JC, Chiu D, Lu M, et al. Agreement and variability in the interpretation of early CT changes in stroke patients qualifying for intravenous rtPA therapy. *Stroke* 1999; 30:1528–1533.
23. Heiss WD. Ischemic penumbra: evidence from functional imaging in man. *J Cereb Blood Flow Metab* 2000; 20:1276–1293.
24. Astrup J, Symon L, Branston NM, Lassen NA. Cortical evoked potential and extracellular K⁺ and H⁺ at critical levels of brain ischemia. *Stroke* 1977; 8:51–57.
25. Phan TG, Wright PM, Markus R, Howells DW, Davis SM, Donnan GA. Salvaging the ischaemic penumbra: more than just reperfusion? *Clin Exp Pharmacol Physiol* 2002; 29:1–10.
26. Mies G, Ishimaru S, Xie Y, Seo K, Hossmann KA. Ischemic thresholds of cerebral protein synthesis and energy state following middle cerebral artery occlusion in rat. *J Cereb Blood Flow Metab* 1991; 11:753–761.
27. Jones TH, Morawetz RB, Crowell RM, et al. Thresholds of focal cerebral ischemia in awake monkeys. *J Neurosurg* 1981; 54:773–782.
28. Heiss WD, Rosner G. Functional recovery of cortical neurons as related to degree and duration of ischemia. *Ann Neurol* 1983; 14:294–301.
29. Sakai F, Nakazawa K, Tazaki Y, et al. Regional cerebral blood volume and hematocrit measured in normal human volunteers by single-photon emission computed tomography. *J Cereb Blood Flow Metab* 1985; 5:207–213.
30. Koenig M, Kraus M, Theek C, Klotz E, Gehlen W, Heuser L. Quantitative assessment of the ischemic brain by means of perfusion-related parameters derived from perfusion CT. *Stroke* 2001; 32:431–437.
31. Wintermark M, Reichhart M, Thiran JP, et al. Prognostic accuracy of cerebral blood flow measurement by perfusion computed tomography, at the time of emergency room admission, in acute stroke patients. *Ann Neurol* 2002; 51:417–432.
32. Klotz E, Konig M. Perfusion measurements of the brain: using dynamic CT for the quantitative assessment of cerebral ischemia in acute stroke. *Eur J Radiol* 1999; 30:170–184.
33. Reichenbach JR, Rother J, Jonetz-Mentzel L, et al. Acute stroke evaluated by time-to-peak mapping during initial and early follow-up perfusion CT studies. *AJNR Am J Neuroradiol* 1999; 20:1842–1850.
34. Miles KA. Measurement of tissue perfusion by dynamic computed tomography. *Br J Radiol* 1991; 64:409–412.
35. Koenig M, Klotz E, Luka B, Venderink DJ, Spittler JF, Heuser L. Perfusion CT of the brain: diagnostic approach for early detection of ischemic stroke. *Radiology* 1998; 209:85–93.
36. Steiger HJ, Aaslid R, Stooss R. Dynamic computed tomographic imaging of regional cerebral blood flow and blood volume: a clinical pilot study. *Stroke* 1993; 24:591–597.
37. Hunter GJ, Hamberg LM, Ponzo JA, et al. Assessment of cerebral perfusion and arterial anatomy in hyperacute stroke with three-dimensional functional CT: early clinical results. *AJNR Am J Neuroradiol* 1998; 19:29–37.
38. Konig M, Banach-Planchamp R, Kraus M, et al. CT perfusion imaging in acute ischemic cerebral infarct: comparison of cerebral perfusion maps and conventional CT findings. *Rofo Fortschr Geb Rontgenstr Neuen Bildgeb Verfahr* 2000; 172:219–226. [German]
39. Mayer TE, Hamann GF, Baranczyk J, et al. Dynamic CT perfusion imaging of acute stroke. *AJNR Am J Neuroradiol* 2000; 21:1441–1449.
40. Cook AJ, Pohlman S, Smith DD, Lin Z. Comparison of contrast injection protocols in CT brain perfusion using two calculation algorithms (abstr). *Radiology* 2001; 221(P):480.
41. Axel L. Cerebral blood flow determination by rapid-sequence computed tomography: theoretical analysis. *Radiology* 1980; 137:679–686.
42. Nabavi DG, Cenic A, Craen RA, et al. CT assessment of cerebral perfusion: experimental validation and initial clinical experience. *Radiology* 1999; 213:141–149.
43. Wintermark M, Maeder P, Thiran JP, Schnyder P, Meuli R. Quantitative assessment of regional cerebral blood flows by perfusion CT studies at low injection rates: a critical review of the underlying theoretical models. *Eur Radiol* 2001; 11:1220–1230.
44. Eastwood JD, Lev MH, Azhari T, et al. CT perfusion scanning with deconvolution analysis: pilot study in patients with acute middle cerebral artery stroke. *Radiology* 2002; 222:227–236.
45. Sorensen AG. What is the meaning of quantitative CBF? *AJNR Am J Neuroradiol* 2001; 22:235–236.
46. Katz DA, Marks MP, Napel SA, Bracci PM, Roberts SL. Circle of Willis: evaluation with spiral CT angiography, MR angiography, and conventional angiography. *Radiology* 1995; 195:445–449.
47. Kirchner J, Kickuth R, Laufer U, Noack M, Liermann D. Optimized enhancement in helical CT: experiences with a real-time bolus tracking system in 628 patients. *Clin Radiol* 2000; 55:368–373.
48. van Hoe L, Marchal G, Baert AL, Gryspeerdt S, Mertens L. Determination of scan delay time in spiral CT-angiography: utility of a test bolus injection. *J Comput Assist Tomogr* 1995; 19:216–220.

49. Blank M, Kalender WA. Medical volume exploration: gaining insights virtually. *Eur J Radiol* 2000; 33:161-169.
50. Prokop M, Shin HO, Schanz A, Schaefer-Prokop CM. Use of maximum intensity projections in CT angiography: a basic review. *RadioGraphics* 1997; 17:433-451.
51. Takahashi M, Ashtari M, Papp Z, et al. CT angiography of carotid bifurcation: artifacts and pitfalls in shaded-surface display. *AJR Am J Roentgenol* 1997; 168:813-817.
52. Rubin GD, Beaulieu CF, Argiro V, et al. Perspective volume rendering of CT and MR images: applications for endoscopic imaging. *Radiology* 1996; 199:321-330.
53. Calhoun PS, Kuszyk BS, Heath DG, Carley JC, Fishman EK. Three-dimensional volume rendering of spiral CT data: theory and method. *RadioGraphics* 1999; 19:745-764.
54. Tomandl BF, Hastreiter P, Rezk-Salama C, et al. Local and remote visualization techniques for interactive direct volume rendering in neuroradiology. *RadioGraphics* 2001; 21:1561-1572.
55. Anderson GB, Ashforth R, Steinke DE, Ferdinandy R, Findlay JM. CT angiography for the detection and characterization of carotid artery bifurcation disease. *Stroke* 2000; 31:2168-2174.
56. Verhoek G, Costello P, Khoo EW, Wu R, Kat E, Fitridge RA. Carotid bifurcation CT angiography: assessment of interactive volume rendering. *J Comput Assist Tomogr* 1999; 23:590-596.
57. Yuh WT, Maeda M, Wang AM, et al. Fibrinolytic treatment of acute stroke: are we treating reversible cerebral ischemia? *AJNR Am J Neuroradiol* 1995; 16:1994-2000.
58. Koroshetz WJ, Lev MH. Contrast computed tomography scan in acute stroke: "You can't always get what you want but. . .you get what you need". *Ann Neurol* 2002; 51:415-416.
59. Ringleb PA, Schellinger PD, Schranz C, Hacke W. Thrombolytic therapy within 3 to 6 hours after onset of ischemic stroke: useful or harmful? *Stroke* 2002; 33:1437-1441.
60. Hamberg LM, Hunter GJ, Maynard KI, et al. Functional CT perfusion imaging in predicting the extent of cerebral infarction from a 3-hour middle cerebral arterial occlusion in a primate stroke model. *AJNR Am J Neuroradiol* 2002; 23:1013-1021.
61. Beauchamp NJ Jr, Ulug AM, Passe TJ, van Zijl PC. MR diffusion imaging in stroke: review and controversies. *RadioGraphics* 1998; 18:1269-1283; discussion 1283-1285.
62. Ueda T, Yuh WT, Maley JE, et al. Current and future imaging of acute cerebral ischemia: assessment of tissue viability by perfusion imaging. *J Comput Assist Tomogr* 1999; 23:1(suppl)S3-S7.
63. Rohl L, Ostergaard L, Simonsen CZ, et al. Viability thresholds of ischemic penumbra of hyperacute stroke defined by perfusion-weighted MRI and apparent diffusion coefficient. *Stroke* 2001; 32:1140-1146.
64. Grandin CB, Duprez TP, Smith AM, et al. Which MR-derived perfusion parameters are the best predictors of infarct growth in hyperacute stroke? comparative study between relative and quantitative measurements. *Radiology* 2002; 223:361-370.
65. Schellinger PD, Jansen O, Fiebich JB, et al. Feasibility and practicality of MR imaging of stroke in the management of hyperacute cerebral ischemia. *AJNR Am J Neuroradiol* 2000; 21:1184-1189.
66. Wintermark M, Reichhart M, Cuisenaire O, et al. Comparison of admission perfusion computed tomography and qualitative diffusion- and perfusion-weighted magnetic resonance imaging in acute stroke patients. *Stroke* 2002; 33:2025-2031.
67. Roberts HC, Roberts TP, Smith WS, Lee TJ, Fischbein NJ, Dillon WP. Multisection dynamic CT perfusion for acute cerebral ischemia: the "togging-table" technique. *AJNR Am J Neuroradiol* 2001; 22:1077-1080.
68. Lev MH, Segal AZ, Farkas J, et al. Utility of perfusion-weighted CT imaging in acute middle cerebral artery stroke treated with intra-arterial thrombolysis: prediction of final infarct volume and clinical outcome. *Stroke* 2001; 32:2021-2028.